School of Civil, Aerospace, and Mechanical Engineering

EXPLOITING THE DEEP LEARNING TECHNIQUE TO STUDY A NOVEL NANO-MODIFIED POLYMER COMPOSITE.

by

Anuradha Mohan Kamble

MSc by Research in Aerospace Engineering

July 2023

Supervisors:

Prof. Ian Hamerton

Dr Carwyn Ward

ABSTRACT

Polymer nanocomposites (PNCs) have gained significant attention in industrial applications due to their enhanced properties compared to traditional composites. These composites incorporate nano-sized particles into a polymer matrix, resulting in improved specific strength properties, weight savings, lightness, and design flexibility. They find applications in various industries, including aerospace, automotive, packaging, and electronics. However, optimizing the properties of PNCs requires a thorough understanding of nanoparticle synthesis, characterization, polymer matrix selection, and nanoparticle dispersion.

In addition to experimental characterisation technics *e.g.* transmission electron microscopy and various spectroscopy technics, modelling and simulation methods, *e.g.* molecular dynamics (MD) simulations, have become indispensable tools in materials science research. However, MD simulations are limited by computing power and simulation time scale, making it challenging to study long-term processes or large systems.

In recent years, there had been a notable rise in data-driven methods such as Deep Learning (DL), Machine Learning (ML), and Artificial Intelligence (AI), and within the field of materials science research. These methods have been applied to analyse experimental and simulation data, enabling the prediction of material properties, classification of microstructures, and identification of processing conditions yet the application of these methods to polymer nanocomposites is still limited, presenting an opportunity for further exploration.

This thesis aims to explore the application of DL techniques to study the phase-separated microstructure of a novel nano-modified polymer composite. The research question focuses on the suitability of DL techniques for this purpose. The objectives include conducting a comprehensive literature review, collecting relevant data on the nano-modified polymer composite, identifying suitable research areas for DL, formulating a problem statement, and investigating the applications of DL techniques for the dataset.

By leveraging DL models, this research aims to provide insights into the phase-separated microstructure of the nano-modified polymer composite, enabling the optimization of its properties. The findings from this study can be useful for future advancements in polymer nanocomposites.

DECLARATION

I declare that the work reported in this thesis adheres to the University Regulations and Code of Practice for Research Degree Programmes. I confirm that this work has not been submitted for any other academic award or recognition. Any collaborative work or assisted work has been appropriately acknowledged and referenced. The opinions and views expressed in this thesis belong solely to the author.

SIGNED: DATE: 4th October 2023

ACKNOWLEDGEMENT

I am grateful to my supervisors, Professor Ian Hamerton and Dr Carwyn Ward, for their invaluable guidance and unwavering support throughout my Masters by Research degree programme.

I am deeply thankful to the Government of Maharashtra for funding my course through the “Rajarshee Shahu” grant. Additionally, I extend my appreciation to the Jean Golding Institute for their support through the "seed corn funding" award.

I would also like to acknowledge the generosity of Professor Jonathan Howse and the Department of Chemical and Biological Engineering at the University of Sheffield. Their permission to utilize their laboratory and their assistance and guidance during the experiments were instrumental in the success of my research. I am grateful for the opportunity to collaborate with the University of Exeter, which allowed me to learn and explore the Fourier-transform infrared (FTIR) and Raman Spectroscopy methods. I extend my thanks to Dr Pascaline Bouzy and Professor Nick Stone for their time and support during my time at the University of Exeter. I would also like to express my gratitude to Dr Germinal Margo and Dr Radhe Shyam for granting me access to the Material Science Laboratory at the Department of Physics (University of Bristol) and for their assistance in the chemical storage and handling. Additionally, I am thankful to Dr Dong Liu, Mr Guanjie Yuan, and Dr Usman Sikander for helping me in experiments of nano-indentation and contact angle measurements respectively.

I am incredibly grateful to my late father for being a source of inspiration. Without his guidance and support, it would have been impossible for me to begin this journey. I want to express my immense appreciation to him for everything I have achieved thus far. I also want to acknowledge the unwavering support of my understanding brother, whose belief in me and constant encouragement kept me motivated throughout. I am grateful to my friends at Hodgkin House, also Muriel and Mervyn supported me in both my triumphs and setbacks during my masters. I would like to extend my heartfelt thanks to my best friend, Damini, for her unwavering support during stressful times. Lastly I’m proud of myself for pushing the boundaries and comfort zone.

AUTHORS CONTRIBUTIONS

The study presented here is accomplished by Anuradha Kamble unless references are indicated. Professor Ian Hamerton (University of Bristol) and Dr Carwyn Ward (University of West of England, Bristol) have contributed by offering their guidance and supervision throughout this study.

Dr Suihua He supplied the initial database of 35 microstructure images out of which 14 unique images were used in the training dataset. Five images mentioned in figure 11 are taken from this dataset. He also helped in developing the section 3.1 Material and 3.2 Blend fabrication method.

Mr Guanjie Yuan has conducted nano-indentation tests under the guidance of Dr Dong Liu and supplied the raw data files generated from these tests. Figure 10 is obtained from the data given by Mr Guanjie Yuan.

Professor Jonathan Howse supervised the experiments conducted at the University of Sheffield for dataset expansion which is reported in Section 6.1 and Section 6.2.

The results and research findings from this study are reported in a journal paper to "Computational Material Science" journal with the title "Exploiting the use of Deep Learning Techniques to Identify Phase Separation in Self-assembled Microstructures with Localized Graphene Domains in Epoxy Blend". This paper was accepted for publication on 10th July 2023.

Contents

LIST OF TABLES

LIST OF FIGURES

LIST OF ABBREVIATIONS AND SYMBOLS

PNC	Polymer Nanocomposite
MD	Molecular Dynamics
AI	Artificial Intelligence
CNN	Convolutional Neural Networks
ReLU	Rectified Linear Unit
FPR	False Positive Rate
TPR	True Positive Rate
ROC	Receiver Operating Characteristic
Adam	Adaptive Moment Estimation
E	Young's Modulus of Elasticity
E_r	Reduced Modulus
E_i	Elastic moduli of Indenter
v	Poisson's ratio
v_i	Poisson's ratio of Indenter
e	Euler's number (2.71828…)
f(x)	Mathematical function with respect to x, where x is input value

CHAPTER 1. INTRODUCTION

1.1 Introduction to polymer nanocomposites (PNCs)

With the increasing demands of industrial applications, material science is constantly advancing. Conventional polymer composites incorporate high-tensile strength reinforcements such as fillers and fibres with excellent modulus into a polymer matrix [1]. The polymer matrix provides toughness and ductility to the composite, while the reinforcement fibres improve the strength, stiffness, and other mechanical properties of the composite. The polymer matrix can be a thermosetting or thermoplastic resin. Thermosetting resins are crosslinked and cannot be melted or reshaped once cured, while thermoplastic resins can be melted and reshaped multiple times. The choice of polymer matrix depends on the application and the required properties of the composite. The reinforcement fibres can be made of a variety of materials such as glass, or carbon. To attain the desired characteristics of the composite material, the fibres are embedded within the polymer matrix with precise orientation and volume fraction. In polymer composite, when subjected to a load, the reinforcement fibres primarily bear the load, while the polymer matrix facilitates load transfer between the fibres, preventing them from buckling or fracturing [1]. This results in a strong and stiff material that can withstand high loads and stress. Consequently, they find wide application in the automobile and aerospace industry.

Polymer nanocomposites (PNCs) are one of the rising innovations in industrial applications [2]. PNCs are composite materials comprising a polymer matrix as the continuous phase and nanoparticles as the dispersed phase. The incorporation of nanoparticles into the polymer matrix imparts remarkable properties to PNCs, including improved mechanical strength, enhanced electrical conductivity, and enhanced optical characteristics. These unique properties have captured the interest of scientists and researchers in recent years, driving significant advancements in PNC. Owing to their improved qualities above conventional composites, they are a topic of interest, *e.g.*, reduction in weight from 20% - 40% with the same specific strength resulting in lightness and design flexibility [3]. Owing to these excellent properties, they have been used in aerospace [4] and microelectronics [5] applications. Additionally, they also offer reduced weight and increased resistance to wear and tear. They achieve these properties by incorporating nano-

sized particles (typically 1-100 nanometres in diameter) into the polymer matrix. These nanoparticles can be clay platelets, carbon nanotubes, graphene, metal oxides, or other materials [6]. The high surface area to volume ratio of nanoparticles means that a small amount of them can significantly improve the properties of the polymer matrix. Additionally, the dispersion of nanoparticles in the polymer matrix can be controlled at the nanoscale, leading to a more homogeneous material with fewer defects. These properties make polymer nanocomposites highly desirable for a range of industrial applications, including aerospace, automotive, packaging, and electronics.

When choosing the nanofillers and polymer matrix, the chemical composition of the components and fabrication process has a significant impact on the properties of polymer nanocomposites, which necessitates multiple iterations to optimize the processing technique [6]. Furthermore, modelling the interaction between nanofillers and polymer matrix is crucial to identify compatible combinations of these components.

The research in PNCs involves these several key areas:

Characterization of nanoparticles: This involves analysing the physical, chemical, and mechanical properties of nanoparticles to understand their behaviour in PNCs [7].

Polymer matrix selection: The selection of an appropriate polymer matrix is critical for the success of PNCs. The polymer should have good compatibility with the nanoparticles, as well as the desired mechanical and thermal properties. [8]

Dispersion of nanoparticles: Achieving an even distribution of nanoparticles in the polymer matrix is a major challenge in PNCs. Several techniques, such as melt mixing, solution mixing, and in-situ polymerization, are used to achieve good dispersion [7].

1.2 Experimental methods used to study polymer nanocomposites

The researchers rely on several experimental technics to study the properties and structure od polymer nanocomposites including the following:

1.2.1 Chemical composition and morphology

X-ray diffraction is used to analyse the structure and morphology of the polymer nanocomposites [9]. It provides information about the crystalline structure and orientation of the nanoparticles in the polymer matrix. Scanning electron microscopy is used to observe the surface morphology of polymer nanocomposites. It provides information on the morphology and distribution of nanoparticles on the surface of the polymer. Transmission electron microscopy is used to visualize the morphology and dispersion of nanoparticles in the polymer matrix [10]. It provides information on the particle size, shape, and distribution within the polymer. Fourier transform infrared spectroscopy is used to analyse the chemical bonding and interaction between the polymer matrix and the nanoparticles [11]. It provides information on the chemical structure and composition of the polymer nanocomposite.

1.2.2 Property measurement

Dynamic mechanical analysis is used to analyse the viscoelastic performance of polymers as well as interfacial interactions concerning temperature and load [12]. It provides information on the effect of nanoparticles on the polymer's mechanical properties. Electrical conductivity measurements are carried out to analyse the electrical properties of thin polymer nanocomposite films. It provides information on the effect of nanoparticles on the polymer's electrical conductivity. Nanoindentation is another powerful tool for understanding the mechanical properties of materials at the nanoscale level such as hardness and elastic modulus [13].

While these experimental techniques provide a wealth of information about materials and their properties, many of the techniques mentioned above require specialized equipment and trained personnel to perform the experiments, which can be expensive. Depending on the technique, sample preparation time, data processing and analysis time can require several hours to days. Therefore, repeating the experiments for slight changes in composition consumes a considerable amount of time and dedicated resources such as equipment cost and specific expertise.

1.3 Modelling and simulation methods

Modelling and simulation methods have become increasingly important in material science research, providing valuable insights into the behaviour of materials. Simulation methods allow researchers to study materials under a wide range of conditions that may not be easily achievable experimentally. For example, Molecular Dynamics (MD) simulations can be used to study materials' behaviour at extreme boundary conditions such as elevated temperatures or pressures [14]. Also, it provides precise control over the conditions under which materials are studied, allowing researchers to isolate and study specific phenomena that may be difficult to observe experimentally. Simulation methods can provide results much more quickly than experimental methods, which saves the required time for sample preparation, data collection, and analysis [14]. This can allow researchers to rapidly test different hypotheses and iterate on their models *e.g.*, changing the composition, *etc.* Detailed data on the behaviour of materials at the atomic or molecular level generated through these simulations can provide valuable insights into the mechanism that controls the material's properties. By combining simulation and experimental approaches, researchers can gain a more comprehensive understanding of the behaviour of materials and design new materials with specific properties for various applications.

Arguably, the most common simulation method in material science is MD simulation, which simulates the movement of atoms and molecules in a material over time. A material is a collection of atoms or molecules, each given an initial position and velocity. To simulate the behaviour of a material, the interactions between the atoms or molecules in the material need to be specified, which are typically described using a mathematical model known as a force field. The force field defines the potential energy associated with different configurations of atoms or molecules in the material, which determines how the material will behave under different conditions. Other simulation methods used in material science include Monte Carlo simulation, which is used to study the thermodynamic properties of materials, and phase field simulation, which is used to study the evolution of phase boundaries in materials [15].

In the context of PNCs, MD simulations can be used to study the behaviour of polymer chains and nanoparticles at the molecular level. For example, researchers can use MD simulations to

investigate the dynamics and diffusion of nanoparticles in a polymer matrix, as well as the mechanical properties of the resulting PNCs.

MD Simulations have applications in other areas such as physics, chemistry, molecular science, and engineering. Early researchers used it to study the kinetics and dynamics of formation and interfacial interactions in such polymers. For example, Güryel *et al.* studied the structure and morphology of three polymer/graphene nanocomposites using classical MD simulations [16]. Similarly, Liu reported that the results from coarse-grained MD simulations for nanoparticle dispersion and aggregation in nano polymer composites imitated the experimental coarsening process and matched with the predicted theory by earlier researchers for polymer filler interaction [17]. This is useful as one does not invest time and money to experiment every time that minor modifications *e.g.*, a slight change in composition, are made.

MD simulations simulate the system under the observation of exceedingly small size (*e.g.*, 10 nanometres) compared to the objects/systems seen or used daily [18]. The number of atoms that can be handled by this simulation also depends upon the complexity of the atomic system, computer power, and software used. MD simulations are limited by the available computing power, and as a result, the simulation time scale is often limited to nanoseconds or microseconds, which can make it difficult to study long-term processes or phenomena that occur on longer time scales [19]. The predictions are accurate for the time scales of period femtoseconds (10–15 s) to nanoseconds [20]. Therefore, simulating large systems such as entire cells or complex materials can be challenging. Additionally, the accuracy of the simulation results is highly dependent on the initial conditions of the system. MD simulations rely on force fields to describe the interactions between atoms and molecules [21]. While these force fields have been developed to accurately describe many systems, they are not perfect, and there is always a degree of error associated with the force field parameters.

1.4 Evolution of data-driven methods

Artificial Intelligence (AI) tools are widely used for image and text-based data in bioscience [22], astronomy [23], and natural sciences [24, 25]. As the field has progressed, its application to materials science has also advanced. The use of machine learning, which is a type of artificial intelligence tool, has been applied in materials science since the late 1990s, primarily due to

advancements in computational power and the accessibility of extensive databases containing materials properties [26]. The application of AI to materials science has accelerated the pace of materials development and opened new opportunities for the discovery and optimization of materials.

Machine learning (ML) is a branch of artificial intelligence that enables computer systems to learn and enhance their performance on a specific task without requiring explicit programming for each step. It involves the use of algorithms and statistical models to enable computers to analyse and make predictions or decisions based on data. The key feature of machine learning is that it uses patterns and insights from past data to inform future decisions or predictions. In ML, a computer system is trained on a dataset that includes input data and corresponding output data. The system uses this data to learn the patterns and relationships between the input and output and then applies this learning to new, unseen data to make predictions or decisions.

Recent studies have investigated the use of AI, ML, and DL methods to help material scientists identify inferences from large experimental and simulation data of microstructures[27-35]. In materials science, the microstructure images and property data generated due to experiments are significant but free access to these data is restricted. A few initiatives, such as the Materials Project [36], Polymer Genome [37], and Open Quantum Materials Database [38], are working towards aggregating, analysing, or visualizing massive quantities of materials research data without any cost. This has contributed to accelerating the applications of ML and DL methods in materials science research.

Significant studies have explored the use of these data-driven methods to study the microstructure of metals and alloys using previous experimental microstructural data. Through the Material Genome Initiative[39] started in 2011, data-driven approaches have led to breakthroughs in the discovery of new glassy materials and better characterization of the glass genome, such as predicting bulk mechanical behaviour from the atomic structure. This is a combined effect of experimental and computational efforts. In another example, a web-based ML model has been designed for real-time screening of thermoelectric material properties [40], saving much time that would otherwise be consumed by manual screening.

Microstructural images from experiments and simulations have been used to develop a data-driven model and train it for a variety of tasks, including predicting properties from microstructure,

classifying microstructures, and determining the processing history of microstructures, among others. Most of these investigations focus on metals [28, 30, 33] and alloys [41, 42] for predicting the mechanical properties, thermal and electric properties, classifying the microstructure, reverse designing the microstructure, *etc.* However, only a limited number of studies have explored such applications of data-driven methods to study the microstructure of polymer nanocomposites [43, 44] and screening of favourable microstructures. By extracting complex patterns and relationships from large datasets, ML algorithms can develop models that predict the properties of polymer nanocomposites based on the properties of their constituent materials and processing conditions. As such, ML is expected to continue to play a vital role in the development of new materials for polymer composites with enhanced properties and performance.

1.5 Thesis introduction

One component in the polymer nanocomposite, which is the polymer matrix, has interesting properties through the controlled phases that can be observed from its microstructure. Phase separation phenomena in polymer blends refer to the separation of distinct phases or components within the material, resulting in a microstructure that is characterized by distinct regions with different physical and chemical properties [45]. This can occur when the polymer matrix is infused with nanoscale fillers or additives. The presence of the fillers can lead to a complex morphology that is difficult to predict or control, but if properly designed, it can result in enhanced mechanical, thermal, or electrical properties.

This phase-separated microstructure has raised significant interest due to its unique morphologies and associated advantages in the microelectronics and aerospace industries [46]. In an earlier study, He *et al*. showcased a technique for producing a multi-component blend which includes a self-constructed bi-continuous phase structure of amine functionalised graphene nanoplatelets (A-GNPs) within the epoxy resin [3]. Wherein, the microstructures developed within the blends lead to exciting enhancements in physical and mechanical properties (*e.g.*, a 103% increase in Young's modulus from 3.2 to 6.3 GPa and a 70% increase in thermal conductivity in domains where the graphene species are localized). However, tailoring the composition to optimize the phase-separated microstructures based solely on experimental techniques is inefficient as it involves multiple iterations of compositions, characterization of resulting microstructure, and property

measurements. This involves a significant number of hours in the laboratory with skilled personnel. Furthermore, due to the complex nature of thermoset systems, confirming the precise mechanism of selectively locating A-GNP within the phase structure of the multi-component blend has proven challenging. Consequently, using the inverse design techniques based on DL could potentially aid in further exploration and comprehension of the underlying mechanism. Hence this thesis explores the DL methods to study the phase-separated microstructure of novel nano-modified polymer composite.

The research question addressed in this thesis is:

"Can we use deep learning techniques to identify the development of phase behaviour in a novel nano-modified polymer composite?"

The research aims and objectives that will help to address this question are:

Research Aim 1: To develop a state-of-the-art review to identify the different areas where DL would be suitable to study a novel nano-modified polymer composite.

Objectives:

➢ To study the past work done on a novel nano-modified polymer composite and collect the data.

Research Aim 2: Identify a suitable area where DL techniques will be helpful to answer the questions related to the novel nano-modified polymer composite.

Objectives:

➢ Analyse the available data and identify the research area of novel nano-modified polymer composite where the DL model is useful.

➢ Form the problem statement for the DL model and select the appropriate DL technique for the given dataset.

Research Aim 3: Evaluate the suitability of the DL model for the problem statement derived from the second research.

Objectives:

➢ Train the model on a variety of data and test its accuracy on unseen data.

➢ Compare the limitations of the given technique and what can be done to overcome them.

To address the research question, the implementation of agile methodology is chosen due to its iterative and flexible nature. The thesis is divided into distinct stages, and after each stage, the output is evaluated to review and make adjustments to the original plan.

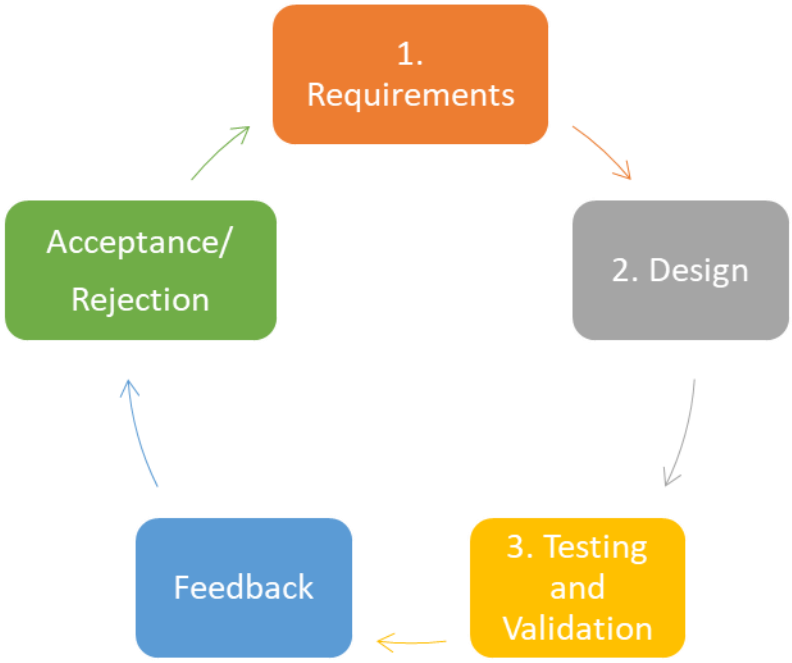

Figure 1. Stages involved in Agile methodology

Based on the literature review and data collection the suitable area for applying DL methods will be identified, which is discussed in detail in Chapters 2, 3, and 4 respectively.

CHAPTER 2. LITERATURE REVIEW

2.1 Introduction

Nanocomposites are composite materials that contain nanoparticles within a polymer matrix, resulting in enhanced mechanical, thermal, and electrical properties. These properties have led to their application in a range of fields, such as electronics, aerospace, and automotive industries. Despite their potential, developing nanocomposites with optimal properties remains challenging, and researchers are exploring novel techniques to improve their performance. In recent years, DL has emerged as a powerful tool for predicting material properties, including those of nanocomposites. This review of the literature examines recent studies that have utilized DL methods to develop novel nanomodified polymer composites and identifies research gaps relevant to this thesis.

2.2 Literature Review Body

2.2.1 Polymer nanocomposites

PNCs are a type of advanced material created by dispersing nanoparticles, such as carbon nanotubes or graphene, within a polymer matrix as shown in Figure 2. As a result, the resulting material gives enhanced mechanical, thermal, and electric properties in comparison to the neat polymer [2, 47, 48]. The advantages of PNCs have led to increased attention in recent years, with a focus on their applications in the electronics, aerospace, and biomedical industries [5, 49, 50].

Polymer nanocomposites are materials composed of a polymer matrix and small nanoscale particles (typically less than 100 nanometres in size) dispersed throughout the matrix [51]. Firstly, the nanoscale particles can act as reinforcing fillers, increasing the stiffness and strength of the polymer matrix [52]. This is because the small size of the particles allows them to distribute more evenly throughout the matrix, providing more points of contact and increasing the interfacial area between the particles and the matrix. This results in improved load transfer and better resistance to deformation, leading to a stronger and stiffer material [6, 53].

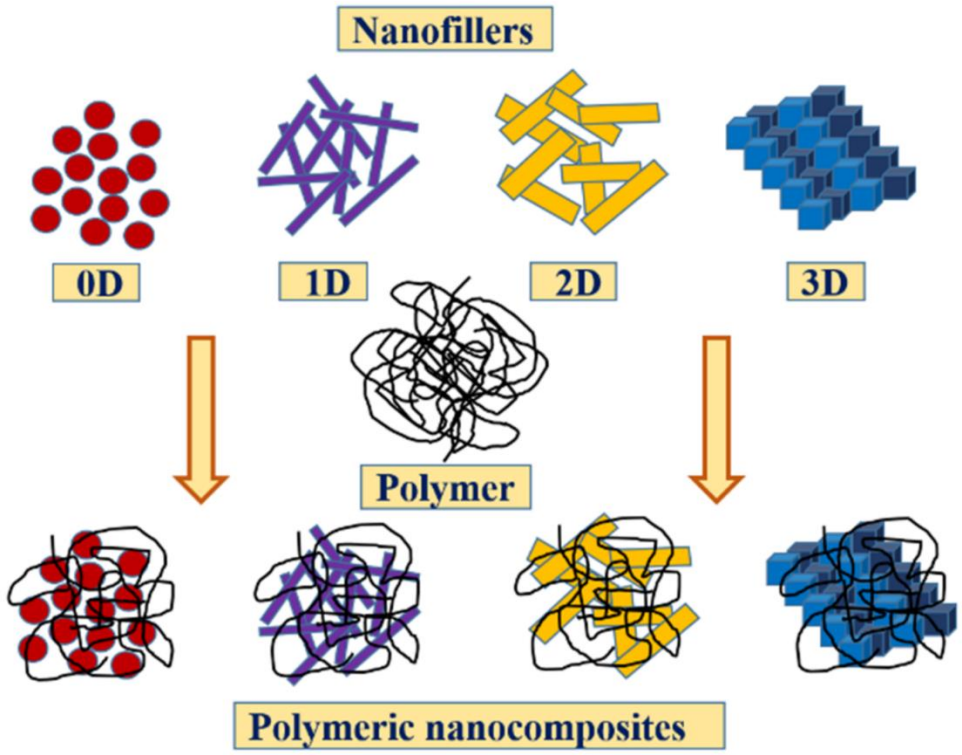

Figure 2. Classification of nanomaterials based on their dimensionality: zero- (0D), one- (1D), two- (2D), and three-dimensional (3D) nanocomposites , image reused with permission from [54]

Secondly, the addition of nanoscale particles can also improve the toughness of the polymer matrix. This is because the particles can act as energy-dissipating sites, absorbing and distributing energy during deformation and preventing the formation of cracks. This can lead to improved resistance to fracture and increased resilience of the material [55]. Furthermore, the addition of nanoscale particles can also improve the thermal stability and dimensional stability of the polymer matrix, as the particles can act as barriers to prevent the mobility and diffusion of the polymer chains [56]. The combination of these factors leads to polymer nanocomposites with significantly improved mechanical, thermal, and electric properties compared to traditional polymer materials. This makes them useful for a wide range of applications in the aerospace, automotive, and electronic industry.

Despite their many advantages, there are still challenges to be overcome in the development and manufacturing of PNCs. One challenge is achieving uniform dispersion of the nanoparticles in the polymer matrix, which can affect the properties of the final composite material. Also, it is reported

that controlling the type and amount of reactive sites on the graphene surface and edges in the polymer matrix has to be studied [57, 58]. Additionally, the manufacturing process of PNCs can be complex and costly, requiring specialized equipment and expertise. The different areas of research in polymer nanocomposites are shown in Figure 3.

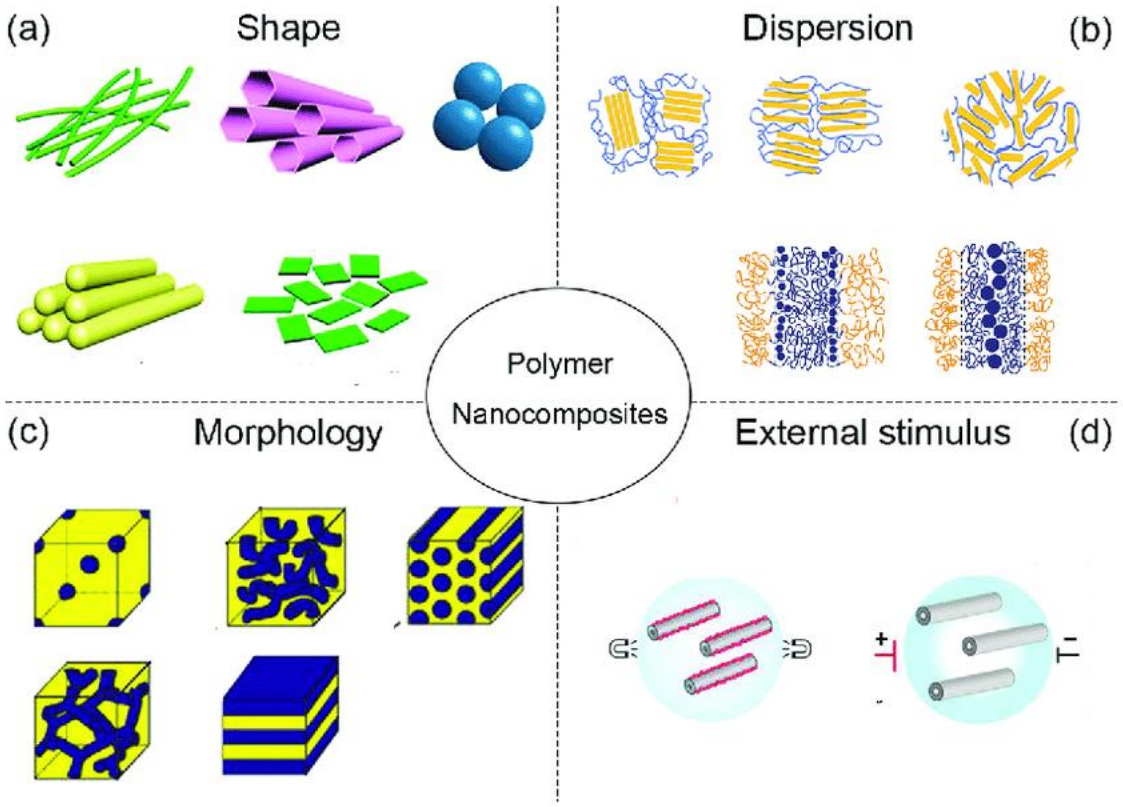

Figure 3. Research areas in polymer nanocomposites, reused with permission [59]

In summary, the need for PNCs arises from their unique properties and potential applications in various industries, including aerospace, automotive, biomedical, and energy. While there are still challenges to be overcome, the development of PNCs has the potential to lead to the development of new advanced materials with improved properties and performance.

2.2.2 Deep Learning

In 1950, Alan Turing posed the question of whether machines can think, which led to the development of machine learning [60]. In the 1950s, Arthur Samuel, an AI pioneer, coined the term "Machine Learning" and defined it as the study of giving computers the ability to learn without being explicitly programmed [61]. Arthur Samuel's self-learning program for a checker

game at IBM was one of the earliest examples of machine learning. AI is increasingly being used in applications such as face recognition, speech recognition, drug discovery, and bioscience research to accelerate the pace of scientific discoveries. The ultimate goal of AI is to create machines that can perform complex cognitive tasks and exhibit human-like intelligence, allowing for quick and efficient completion of tasks that would otherwise be time-consuming and resource-intensive. For instance, screening a dataset of thousands of materials to select the ones with excellent properties for energy storage applications would be a time-intensive task for humans, with a risk of manual errors. By using AI tools, researchers can save time and resources and focus on the critical aspects of research that require human creativity and critical thinking for problem-solving.

Machine learning is a branch of artificial intelligence that utilizes algorithms to analyse data, identify patterns, and use that information to make predictions on new data. In the context of material science, researchers can train machine learning models on datasets of structure-property relationships, enabling the models to learn from the data and predict the properties of materials under different conditions, such as temperature, pressure, or stress, based on their intended applications and available data [62, 63]. This approach can aid in the design of materials that possess increased resistance to extreme conditions or exhibit specific properties under certain conditions.

DL is a subfield of machine learning that falls under the umbrella of Artificial Intelligence as shown in Figure 4. It employs artificial neural networks with multiple layers to learn from hierarchical representations of data. LeCun's paper on the application of convolutional neural networks for image and speech recognition was the first to demonstrate how the networks could automatically extract features from images, as opposed to requiring manual feature extraction as in traditional machine learning [64, 65]. Qu applied deep neural networks to quantify the states of nanoparticle assembly in polymer matrices using transmission electron microscopy (TEM) images, a task that is difficult to accomplish with only visual inspection [66]. While most studies in material science have used DL methods, they are focused on the microstructures of metals [28, 30, 33] and alloys, and only a few [44] have examined polymer nanocomposites.

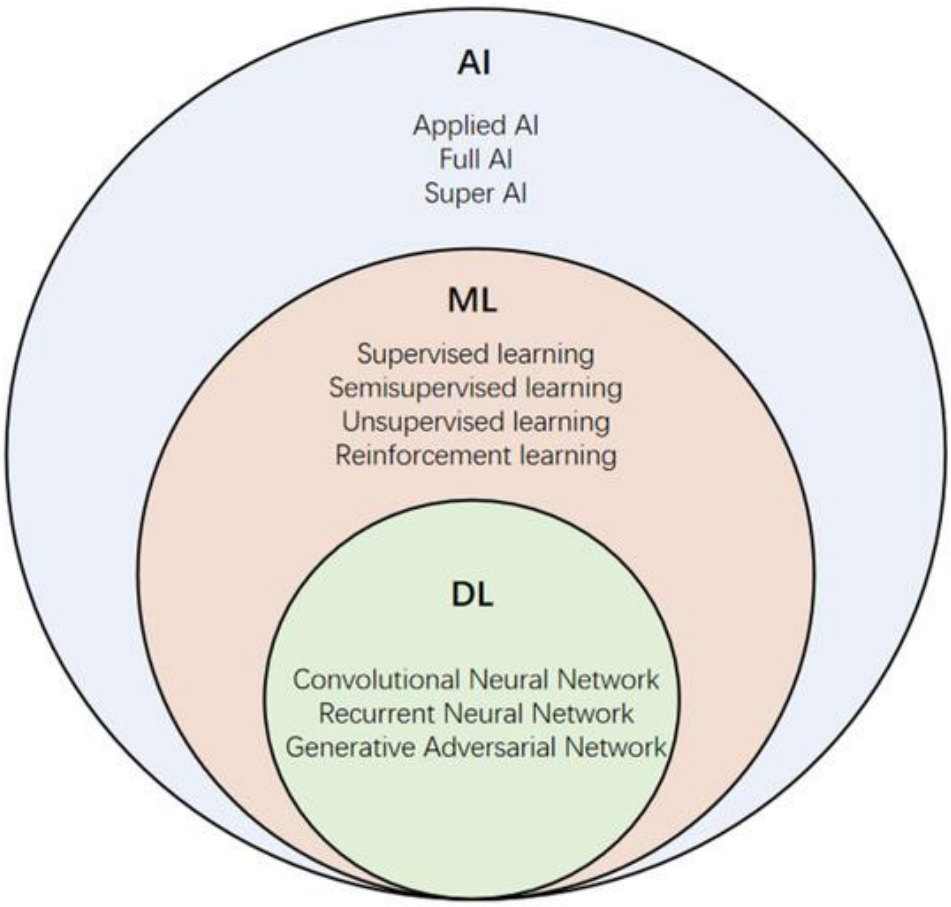

Figure 4. AI, ML and DL in relation to one, reused with permission [67]

In machine learning, a model can be thought of as a function that maps inputs to outputs. For example, in a simple linear regression model, the relationship between input variables and output variables is represented by a linear equation.

A specific model could be the VGG16 model [68]. VGG16 is a DL model and it is pre-trained on ImageNet which is a huge image database. It consists of multiple convolutional and fully connected layers, which learn to extract hierarchical features from images and make predictions about their classes. VGG16 can be considered a model because it represents a specific implementation of the CNN algorithm for image classification tasks. Some commonly known models in machine learning are linear regression, logistic regression, random forest, and neural networks. The model selection in DL depends upon the problem statement and the characteristics of the datasets.

Typically, a neural network comprises three layer types: the Input Layer, Hidden Layer(s), and Output Layer. The primary function of the input layer is to hold the input data, devoid of any calculations. It is necessary to use the non-linear activation function in hidden layers. This is crucial for introducing non-linearity, enabling the network to effectively learn intricate patterns. Neglecting non-linear activation functions would result in a neural network with multiple hidden layers that resembles a large linear regression model, rendering it incapable of effectively learning complex patterns from real-world data. The performance of a neural network model exhibits significant variation based on the type of activation function employed within the hidden layers. Moreover, an activation function must also be employed in the output layer of a neural network. The specific choice of activation function is contingent upon the type of problem one intends to solve.

Model Architecture refers to the overall design or structure of a model. It encompasses the choices regarding the type and number of layers, the connections between layers, and the activation functions used. The activation function decides whether the output of the layer is useful or not. There are different activation functions. As an example, the famous VGG16 model consists of 13 convolutional layers, followed by three fully-connected layers and a SoftMax layer for classification [68].

DL relies on available data to train the models. In material science, material properties are influenced by various factors such as microstructure, processing conditions, and atomic/molecular structure. The training data for the models are obtained from experiments and they includes microstructural and compositional information as well as properties under varying conditions such as temperature and pressure. CNN is used in image-related tasks due to its ability to effectively capture spatial dependencies and extract meaningful features from images [69] such as investigation of microstructure. However, the data collected are often heterogeneous due to the different processing parameters and microstructures of the materials studied [39, 63].

DL is employed in solving complex problems where the data is non-uniform and automatic feature extraction is necessary, such as crystal structure prediction [70]. With the recent advances in the semiconductor industry, computational power is readily available, making it possible to support big data exploitation. Polymer films have been widely used in energy storage, coating, wearable

gadgets, and aerospace applications [5, 49, 71-75]. The studies conducted during 2015-2020 for applications of DL in material science explore the prediction of mechanical, electrical, and thermal properties from the microstructure using tools of artificial intelligence [44, 76-78]. In 2015, Pyzer-Knapp *et al.* stated that high-throughput virtual screening would be a critical aspect of material science [79]. In 2016, Cang attempted to extract and reconstruct complex microstructures of tin and lead-based alloys using a convolutional deep belief network [31].

2.2.3 Deep learning for PNC

Fortunately, the rise of advanced imaging techniques providing high-resolution, such as atomic force microscopy (AFM), scanning tunnelling microscopy (STM), and scanning transmission electron microscopy (STEM) has enabled researchers to observe and understand the microstructure relating to its properties and behaviour. These methods help researchers to study the material on micro level. Up to this point, material science has utilized simulated microstructure images for image recognition-based tasks due to limited access to past research data. However, as simulated data may not accurately represent the real conditions in experimental data, the precision of DL may contain deviation from actual results through experimentation. By integrating high-resolution real-world image data with DL, it is possible to gain valuable insights into chemical history, phase transitions, and other related phenomena from microstructures. The overview of the working of the DL method is shown in Figure 5.

The proposed method utilizing DL has been proven effective in predicting the electromechanical properties of complexly structured PNCs, as demonstrated by the evaluation results [43]. This success can aid in the development of new PNCs with optimized properties. In another study, a convolutional neural network (CNN) has been utilized to analyse transmission electron microscopy images of PNCs and accurately identify the nanoparticle assembly states [66]. CNN was trained on a dataset of TEM images of PNCs with known assembly states and was able to classify new TEM images into their corresponding assembly states with precision.

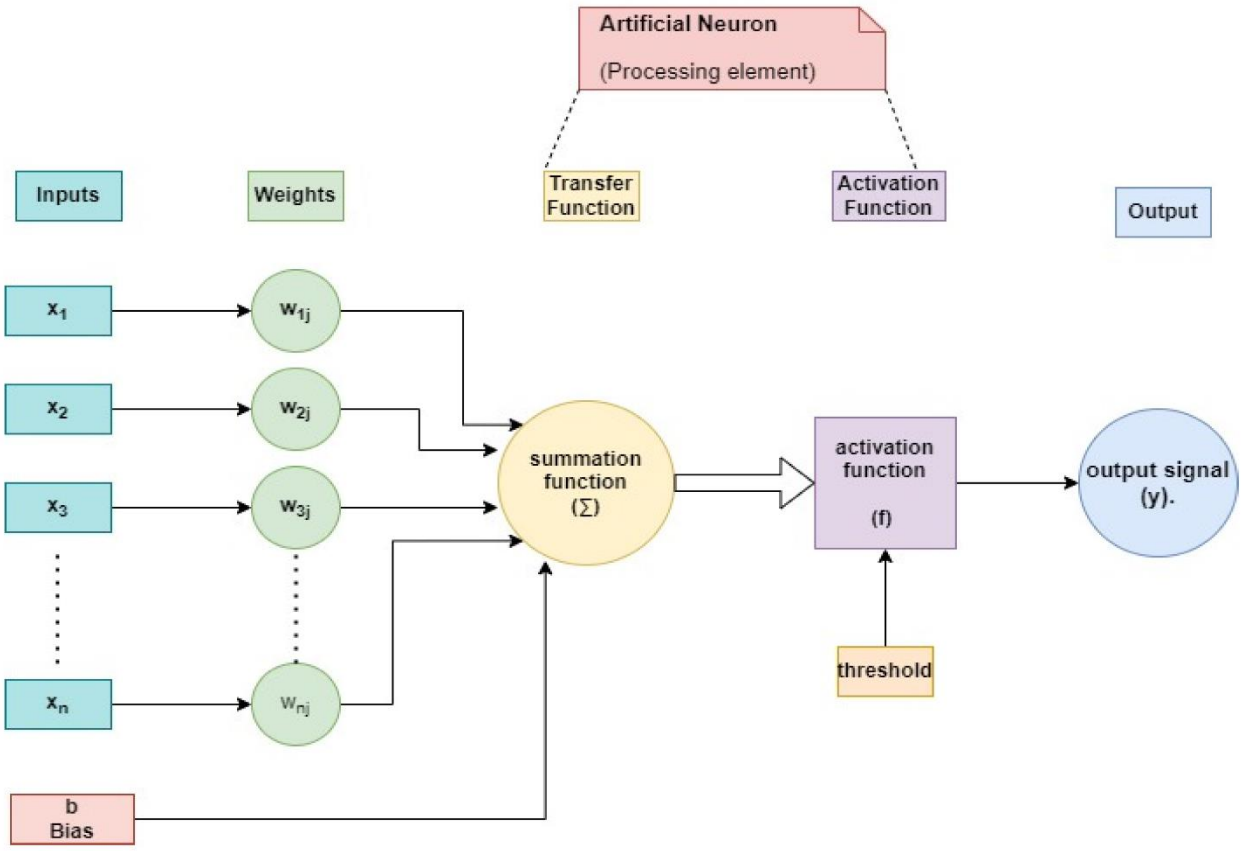

Figure 5. Steps involved in building DL model, figure used with permission [80]

In their research paper, Zazoum *et al.* investigated the effectiveness of deep neural networks (DNNs) in modelling the mechanical properties of these nanocomposites [81]. The researchers created a DNN model based on experimental data to predict the tensile strength and modulus of elasticity of the material. The study concluded that the DNN model performed well and accurately predicted the mechanical properties of the nanocomposites. These findings suggest that DNNs can be a valuable tool in designing new materials with optimal mechanical behaviour for various applications. The paper emphasizes the potential of using DNNs in modelling and predicting the properties of complex materials.

The article discusses the use of various DL techniques for applications in polymer, polymer composite chemistry, structures, and processing [82]. The authors provide an overview of DL techniques and their potential applications in polymer science and engineering. The article highlights the use of DL for predicting the properties of polymers and polymer composites, such as tensile strength, modulus of elasticity, and glass transition temperature. It also discusses the use

of DL for optimizing polymer processing parameters, such as melt temperature and cooling rate. The authors also discuss the power of DL for predicting the structure of polymers and polymer composites, including molecular structure, morphology, and crystallinity. They highlight the application of DL for image analysis and segmentation, which can aid in the characterization of complex polymer structures. Overall, the article demonstrates the potential of DL for advancing the field of polymer science and engineering. The use of DL techniques can help researchers and engineers to design and optimize new materials and processes, and to investigate the behaviour of complex polymer systems.

The article by Demirbay *et al.* describes a study on the use of deep neural network (DNN) classifiers for classifying the opacity of polymer nanocomposite films [83]. The researchers developed DNN models based on experimental data to classify the films into three opacity levels: transparent, translucent, and opaque. The study found that the DNN classifiers were able to accurately classify the opacity of the films, with an overall accuracy of over 90%. The results suggest that DNN classifiers can be a valuable tool for rapid and accurate classification of the opacity of polymer nanocomposite films, which can aid in the development of new materials with specific optical properties. The article also discusses the potential of using DNN classifiers for other applications in polymer science and engineering, such as predicting the mechanical properties and thermal stability of polymer composites. The authors suggest that DNN classifiers could be combined with other modelling and simulation techniques to enhance overall comprehension of the behaviour of complex polymer systems. Overall, the article demonstrates the potential of using DNN classifiers for classification tasks in polymer science and engineering and suggests that they could be a valuable tool for optimizing the properties and performance of advanced polymer materials.

In their research, Jiang *et al.* (2020) explored the potential of DL techniques for predicting the mechanical properties of nanocomposites [84]. The researchers developed a deep neural network that could predict the tensile strength and modulus of carbon fibre-reinforced polymer composites with different types and amounts of nanoparticles. The model achieved high accuracy and was able to identify the optimal nanoparticle content for the highest mechanical strength.

Liu *et al.* (2021) presented a hybrid machine-learning model for predicting the thermal conductivity of graphene-based nanocomposites [85]. The researchers used a convolutional neural

network to analyse the microstructure of the composite and predict the thermal conductivity. He reported that the results from coarse-grained MD simulations for nanoparticle dispersion and aggregation in nano polymer composites imitated the experimental coarsening process and matched with the predicted theory by earlier researchers [86] for polymer filler interaction.

Liu *et al.* (2021) developed a deep-learning model to predict the fracture toughness of epoxy composites reinforced with carbon nanotubes. The researchers used a neural network with multiple hidden layers to analyse the stress-strain curve of the composite and predict its fracture toughness. The model showed good accuracy and was able to predict the fracture toughness of the composite with high precision.

It is important to note that the applications of DL models in material design have not been fully exploited. For instance, the features extracted by deep convolutional networks or other unsupervised DL models have yet to be combined with processing conditions and material properties to establish predictive models. Further exploration in this area is recommended [29].

Based on recent research in polymer nanocomposites it is observed that DL is a useful method to analyse the pattern from microstructure and predict the structure-property relationship. The polymer nanocomposite developed which has shown improved mechanical properties needed further analysis into its phase microstructure. Therefore, the DL method is chosen to investigate whether it's suitable for studying the modified polymer nanocomposite.

2.3 Summary of the findings

The studies discussed above demonstrate the potential of DL techniques for studying the microstructure of complex materials such as polymer nanocomposites. These techniques have the advantage of being able to analyse large amounts of data and identify complex relationships between the different components of the composite. The novel nano-modified polymer composite has the potential to be used as a coating in electronics applications.

However, more research is needed on the microstructure of this new PNC, which gives exceptional mechanical and thermal properties. The utilization of data-driven methods has accelerated research in polymer nanocomposites due to their efficiency and cost-effectiveness compared to experimental characterization and simulation methods. Therefore, it is important to investigate the

validation of these DL techniques. DL techniques provide the means to examine the microstructure insights of newly developed polymer nanocomposites. Therefore, the research question introduced in Chapter 1 concentrates on this area and seeks to advance the implementation of DL for newly developed PNCs. This fulfils the first research aim of this study.

For microstructure studies, the earlier research has been carried out using convolutional neural networks (CNN) which is a type of artificial neural network used in DL. They have proven effective in extracting the features from images in computer vision and image recognition tasks. Hence the DL model used for answering this question is selected as CNN.

The first step will be data collection through contacting the established researchers in this field who have studied the polymer nanocomposites. Subsequently, a rigorous analysis will be conducted to finalise the precise problem statement suitable for the CNN model, such as property prediction or classification. Following this, the model will be designed and implemented. It will then undergo a rigorous training and testing steps to assess its efficacy in solving the identified problem. The investigation will be done on the model's performance and corrective measures and methods will be applied to enhance the performance of model by reviewing the literature. Finally, a comparative analysis with existing literature will be undertaken to affirm the model's validity and its potential application in advancing the study of novel nano-modified polymer composites.

CHAPTER 3. MATERIALS AND METHODS

Given their wide-ranging applications in coatings, electronics, and adhesives, epoxy resins emerge as pivotal choices for crafting polymer nanocomposites [87]. Within the epoxy resin system, the hardener functions as a curing agent, initiating a chemical reaction with the epoxy resin to yield a robust, thermosetting material characterized by a three-dimensional crosslinked structure. Notably, amine-based curing agents are deployed in tandem with epoxy resins to augment mechanical properties and furnish critical corrosion protection, particularly salient in applications like wind turbine coatings.

The selection of resins is additionally influenced by their processing temperature range, an attribute with direct bearing on the kinetics of the curing process. Consequently, RS-M135, distinguished by a processing temperature range of 10°C to 50°C under standard room conditions, emerges as the epoxy resin system of choice for this study. This system is judiciously paired with hardeners RS-MH134 and RS-MH137, aligning with demands of boat and shipbuilding, as well as energy turbine blade applications.

The most extensively researched nanofillers for reinforcement purposes encompass clay (specifically montmorillonite MMT), carbon nanotubes, and graphene. The research domain commenced with polymer-clay nanocomposites in the late 1980s, followed by the exploration of polymer-carbon nanotube nanocomposites in the late 1990s. Since the seminal discovery of graphene in 2004, and its extraordinary elastic modulus of 1.1 TPa [88] and a noteworthy thermal conductivity of approximately 4000 W$m^{-1}K^{-1}$ [89] it has catapulted it into the realm of polymer nanocomposites. Homogeneous dispersion of the nanofiller in the polymeric matrix and strong interaction between the filler and the polymer is absolutely necessary for good reinforcement. Nanotubes that undergo covalent functionalization offer superior polymer reinforcement, facilitating improved stress transmission between the polymer matrix and the nanofiller. Nonetheless, it is worth noting that covalent functionalization has the potential to compromise the innate electrical properties of CNTs. [90], necessitating an elevated percolation threshold. The electrical percolation threshold designates the crucial concentration of reinforcement at which the composite undergoes a sudden transition from being an insulator to becoming a conductor, owing to the emergence of conductive pathways. Homogenously dispersed graphene also reduces barrier

properties. Conspicuously, amine-functionalized graphene nanoplatelets (A-GNPs) within the polymer matrix have been observed to engender a bi-continuous phase-separated microstructure, where this phase shows excellent mechanical strength, thermal conductivity and electrical conductivity. Consequently, in this study, in concert with the aforementioned epoxy resin system, A-GNPs have been selected as the nanofiller of choice due to its superiority in satisfying functional requirements in commercial applications.

3.1 Materials

The material was originally examined in the publication of He *et al.* [3] and the same compositions are employed in this work. Three main constituents were used to prepare the blend. Constituent 1 is Epoxy resin, RS-M135. Constituent 2 is RS-MH137, which is a curing agent. Both of these constituents were delivered by PRF Composites UK. Constituent 3 is 1-(2-aminoethyl)piperazine (AEPIP) (CAS No. 140-31-8) and it was supplied by Sigma Aldrich. Amine-functionalized graphene nanoplatelets (A-GNPs) (mean diameter - 2 μm, thickness < 4 nm) were supplied by Cheap Tubes Inc., USA. These constituents are used in the same condition as delivered without any modifications.

In addition to the commercial materials used above, other consumables were used which were taken from standard laboratory setups and these involved glass slides, Acetone, a magnetic stirrer, a storage container for chemicals and a slide holder. The glass slides were supplied by Fisherbrand. Acetone (GPR) was purchased from Sigma Aldrich and distilled water was produced in house and were used to clean the glass slides, which were dried using a vacuum line.

3.2 Blend Fabrication Method

The GNPs were dispersed in the curing agent *via* sonication using a "GT Sonic" ultrasonic water bath. The epoxy resin was degassed using a vacuum pump (5.25 mmHg, for 10 min). Epoxy to curing agent was mixed in the proportion of 1:1 (weight in grammes) to 1:9 (weight in grammes); a Precisa 205 A, the weighing scale was used for weighing these materials in required quantities. The GNPs (3 wt.%) were dispersed in the curing agent using a sonication probe at room temperature for 1 hour. This mixture was then added to the degassed epoxy at different ratios to prepare the multiple blends with varied microstructures. The second set of experiments was

designed such that keeping the hardener to epoxy ratio constant and varying the ratio of graphene nanoplatelets (GNPs) *e.g.*, epoxy (3): curing agent (1) while the GNP content was varied from 1% to 10% of the total weight of the blend. In the second scenario, the ratio of epoxy to curing agent is varied and the ratio of GNP was kept constant *e.g.*, epoxy (3): curing agent (1 –10): GNP (3% of the weight of the blend). The ratio of GNP in the curing agent was varied from 1% to 10% by weight of the total blend. Once the GNPs were dispersed in the curing agent, the mixture was added to the epoxy resin and the resulting polymer blend was stirred manually for 10 min to ensure proper mixing. The glass slides were cleaned with acetone followed by diluted water. Then the glass slide was properly dried using the N_2 gas line. The A-GNP composite film was fabricated on the clean and dry glass slide using the spin coating method. The glass slide was placed on the spin disk and the quantity of blend to be placed on the glass slide was measured by the 100ml pipette. The spin coater was maintained at a spin speed of 1500 rpm for 1 minute for all the samples. Subsequently, the film was post-cured by keeping it in the oven at 50°C for 5 hours.

3.3 Data Acquisition Method

The samples were then observed using the Leica optical microscope at 10x magnification as shown in Figure 6. The raw images were captured using Twain software without any modifications.

Figure 6. a) Image acquisition using an optical microscope at the University of Bristol during the first set of experiments.

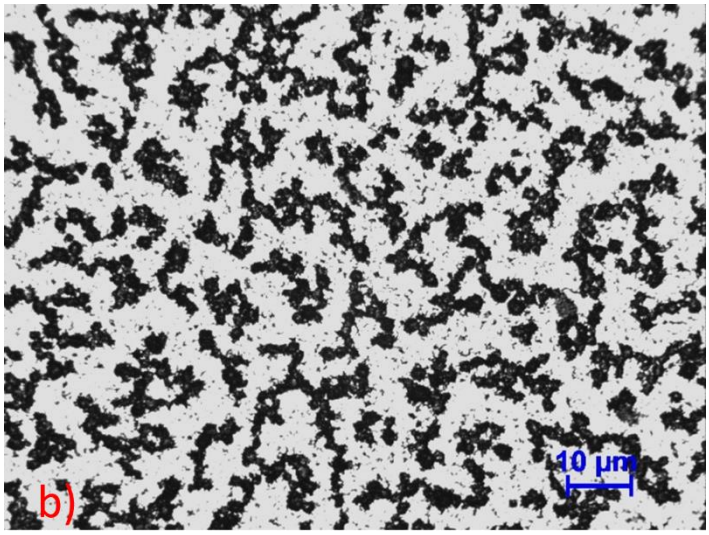

Figure 6. continued b) Observed microstructure.

3.4. Property Measurements

3.4.1 Mechanical Property measurement

Nanoindentation is a materials testing technique used to assess mechanical properties, such as hardness and elastic modulus, at the nanoscale. It involves applying a controlled load to the surface of a material using a sharp indenter, typically a diamond or a hard tip with known geometry, while simultaneously monitoring the depth of penetration into the material. During the test, a load is gradually increased and then decreased while continuously recording the depth of penetration or displacement. The indentation depth is typically in the range of a few nanometres to several micrometres. The hardness of the material is determined from the maximum load applied during indentation divided by the projected contact area between the indenter and the material surface. It represents the material's resistance to plastic deformation and is a measure of its ability to withstand localized applied forces. By analysing the load-displacement data, various mechanical properties of the material can be extracted [13, 91]. The loading and unloading curves are shown in Figure 7 given below.

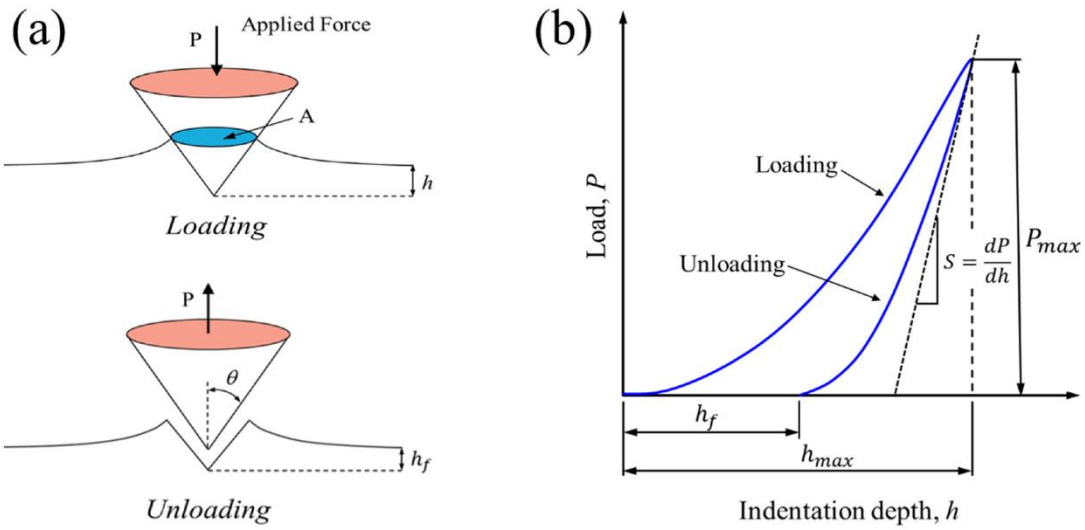

Figure 7. (a) A schematic representation of loading and unloading in indentation tests. (b) Typical indentation load–depth curve with important measured parameters, image used with permission from [92]

The loading time, holding time, and unloading time for all the samples are 5 seconds, 3 seconds, and 5 seconds respectively. The samples used for the testing were obtained from a previous PhD study [3]. The nanoindentation tests were carried out by Mr. Guanji Yuan who is pursuing PhD at the University of Bristol and the raw data files generated from the tests were supplied by him. The post processing of the data, to find out the Elastic Modulus or Young's Modulus of Elasticity, was performed using the equation 1. 15-20 measurements were taken for each sample and the mean of those measurements is considered to be the final value of Young's modulus.

The Young's modulus (E) of the sample was calculated using equation 1 [93, 94],

$$\frac{1}{E_r} = \frac{1-\nu^2}{E} - \frac{1-\nu_i^2}{E_i} \qquad \text{Equation 1}$$

where, E_i (1140 GPa) and ν_i (0.07) are the elastic moduli and Poisson's ratio of the diamond indenter [94]. The value of Poisson's ratio ν (for the epoxy was taken as 0.34 from the literature). [95] The polymer blends differ from each other by their composition. Hence the corresponding microstructure had a different elastic modulus (MPa).

3.4.2 Contact Angle Measurement

Wettability is the ability of a liquid to maintain contact with a solid surface. A contact angle (θ) is a thermodynamic property that indicates the wettability of a solid surface [96]. The contact angle is the angle formed by a liquid at the three-phase boundary where a liquid, solid, and gas interact [97]. The higher the contact angle lower is the wettability. Wettability is useful in thin film fabrication as If a liquid droplet spreads over a given solid surface it means the wettability is higher and thus lower contact angle as shown in Figure 8 given below. In the case of perfect wetting, the θ (theta) is 0°. The surface tension of a liquid and the surface energy of the solid surface play crucial roles in determining wetting behaviour. If the surface energy of the solid is similar to, or lower than, the surface tension of the liquid, the liquid will tend to wet the surface and spread out. However, if the surface energy of the solid is higher than the surface tension of the liquid, the liquid will have a higher contact angle and less wetting. This serves as a valuable tool for determining the compatibility of a solid surface for fabricating the blend.

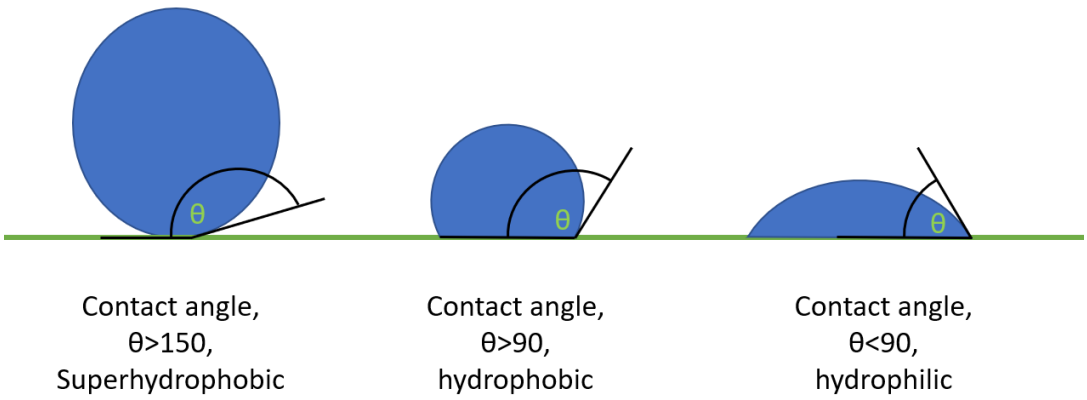

Figure 8. Schematic showing the relation between the contact angle and wettability of the droplet with a solid surface

To investigate the wettability of the neat epoxy blend and nano-indented polymer blend, contact angle testing was performed using the sessile drop method with the assistance of DSA 100 (Drop Shape Analyzer – Krüss DSA). The sessile drop method was selected and the fitting method employed to measure the contact angle of the drop was Ellipse. After placing the glass slide coated with the neat epoxy film onto the stage or nano-modified polymer blend the stage was manually

calibrated. A micro syringe, controlled by the software, was used to slowly place a drop of distilled water onto the glass slide. Approximately 20-25 contact angle measurements were recorded for both cases and the mean value, along with the standard deviation, was calculated based on these measurements. The experimental setup is shown in Figure 9.

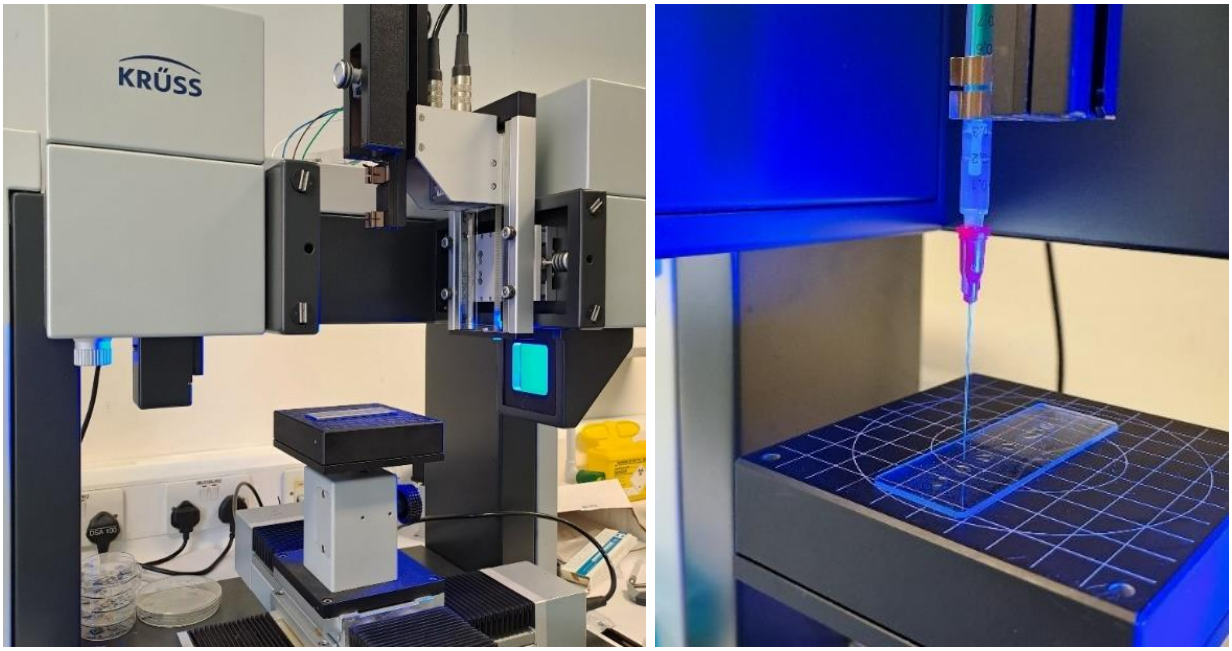

Figure 9. Experimental setup for contact angle measurements using DSA 100.

3.5 Summary

In conclusion, the Young's modulus of the five samples was measured through nanoindentation tests. This was done in collaboration with the Department of Physics at the University of Bristol. For every sample 15-20 measurements were carried out and mean of those values is used to determine the Young's modulus of every sample. The results of these tests are shown in the next chapter which compares the microstructure with the resulting value of Young's modulus.

The wettability of the neat epoxy polymer film and the nano-indented polymer film was evaluated using Drop Shape Analyzer – Krüss DSA for the contact angle measurements. The findings from these tests will be comprehensively discussed in the subsequent chapter, Chapter 4.

CHAPTER 4. EXPERIMENTAL RESULTS

4.1 Nano-indentation testing

The 5 samples are tested for nano-indentation. For reference, the area that was subjected to testing can be seen in Figure 10. The black region with A-GNPs was assumed to have higher mechanical strength compared to the white region surrounding it. Equation 1, mentioned in Chapter 3, was used to calculate the Young's modulus. The blend compositions and respective Young's moduli are shown in Table 1 and the associated microstructure is shown in Figure 11.

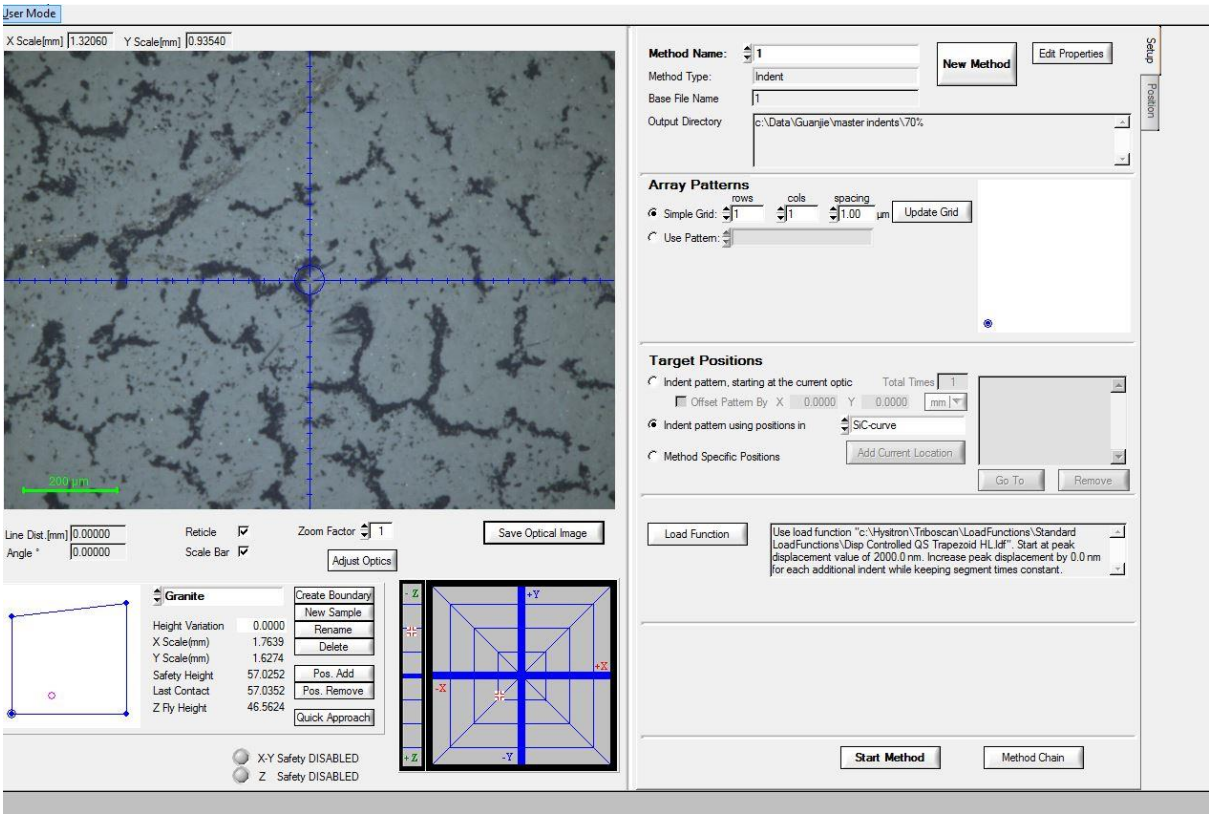

Figure 10. Nano-indentation test set up carried out by PhD researcher, Mr Guanjie Yuan from the Department of Physics at the University of Bristol.

Table 1. Nanoindentation test results

Nano Indentation Test results			
Sample name	The ratio of epoxy: hardener	Young's Modulus (Gpa)	Standard deviation
a.	90:10	**5.8**	**0.7**
b.	80:20	**5.0**	**0.5**
c.	50:50	**8.8**	**0.8**
d.	70:30	**6.2**	**1.8**
e.	100:0	**3.0**	**0.6**

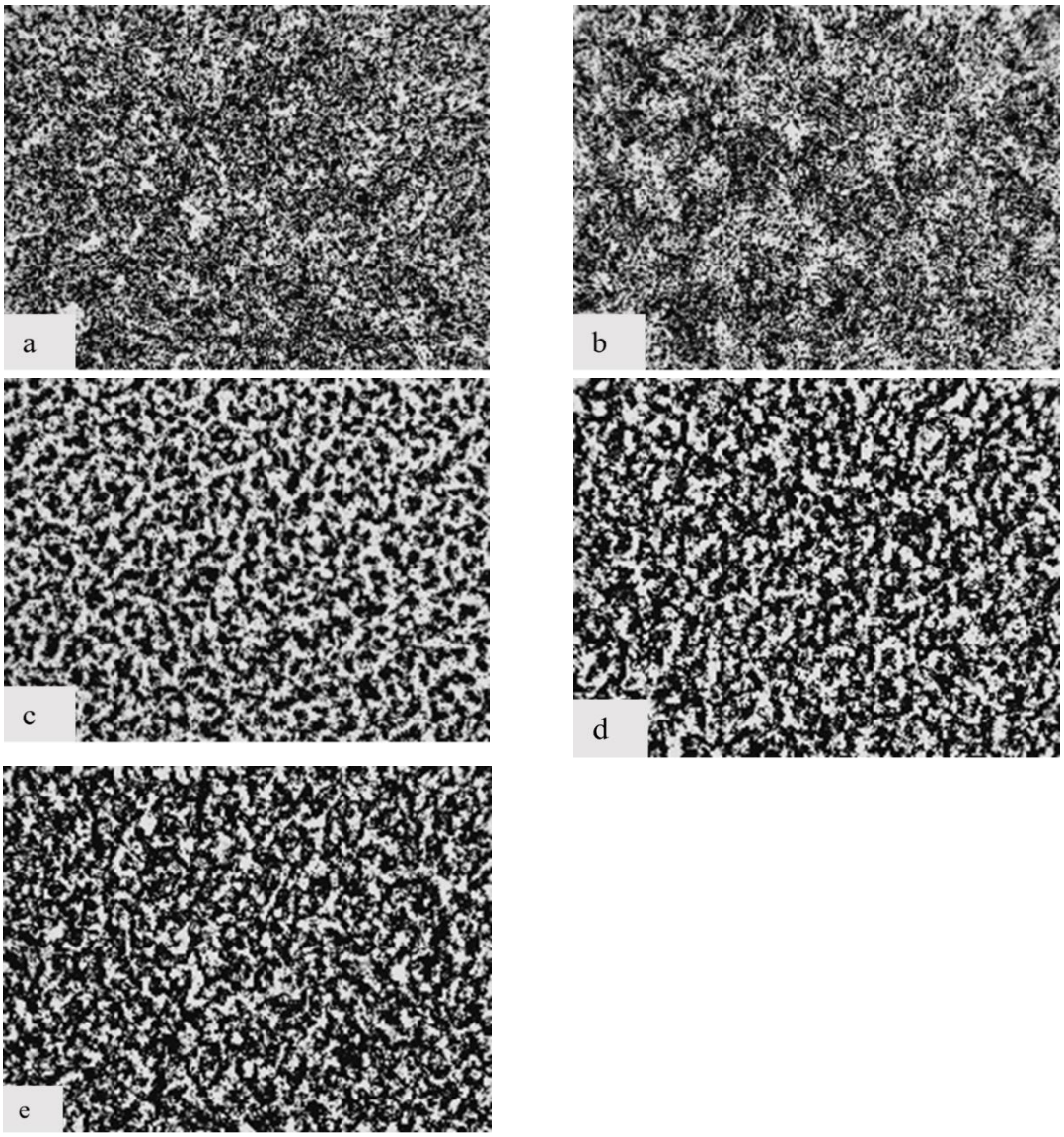

Figure 11. Microstructures of the following blends are named a), b), c), d) and e) as mentioned in Table 1. (The images are used with permission [3])

The sample which contained an epoxy: hardener ratio of 50:50 showed an enhanced Young's Modulus *i.e.* 8.8 Gpa against others. Even though there is enhancement in the mechanical property, the resulting range of Young's modulus is between 3 Gpa – 8.8 Gpa from the lowest to highest possible composition change. Farizhandi *et al.* [98] in their research of predicting chemistry and processing history from microstructure using DL predicted the temperature range from 853 – 963 °C*i.e.* a wide range of values. In other research, Kirklin *et al.* [99] used DL to predict the formation energy (eV/atom) of 1670 materials ranging from 0.096 to 0.136 eV/atom for the Open Quantum Materials Database (OQMD). The lowest dataset size reported for property prediction of materials is 100-500. Therefore, the dataset presented in the present work is limited as the set composition gives a unique microstructure (*i.e.* there are 5 such different microstructures with corresponding mechanical properties). There is little change in microstructure with respect to change in composition from 10% - 100% which limits the present dataset size for property prediction. Therefore, the scope of DL for property prediction of novel nano modified polymer composite is limited and cannot be explored any further.

4.2 Contact angle measurements

The drop of distilled water placed on a neat epoxy-coated glass slide was captured using the software DSA 100, as depicted in Figure 12. For both cases, the sessile drop template was selected, and the Ellipse fitting method was utilized to measure the contact angle of each drop. A total of 21 measurements were conducted to determine the contact angle of the neat polymer film, and these measurements are illustrated in Figure 13. The mean and standard deviation of the observations were calculated and presented in Table 2. The measurements were performed at a room temperature of 20°C. The recorded mean contact angle for the neat epoxy polymer film is 32.98°, indicating its hydrophilic nature.

Table 2. Contact angle measurements of neat epoxy blend

Parameters	Value	Standard deviation
Mean diameter [mm]	4.25	0.44
Mean volume [µL]	4.46	1.20
Mean contact angle [°]	32.98	1.98

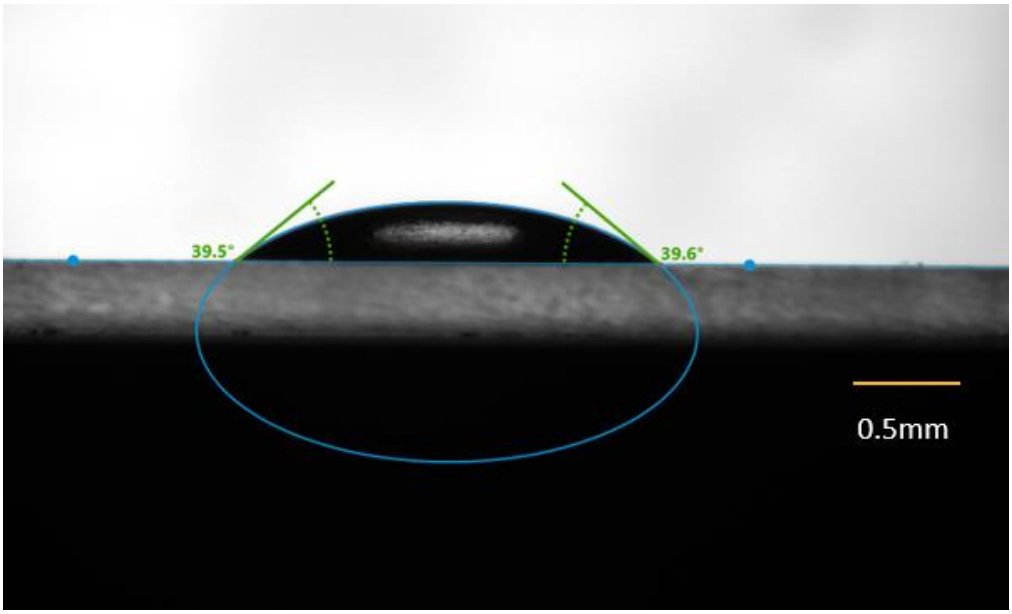

Figure 12. A drop of distilled water is placed on a neat epoxy-coated glass slide for contact angle measurement using the KRÜSS DSA 100 instrument.

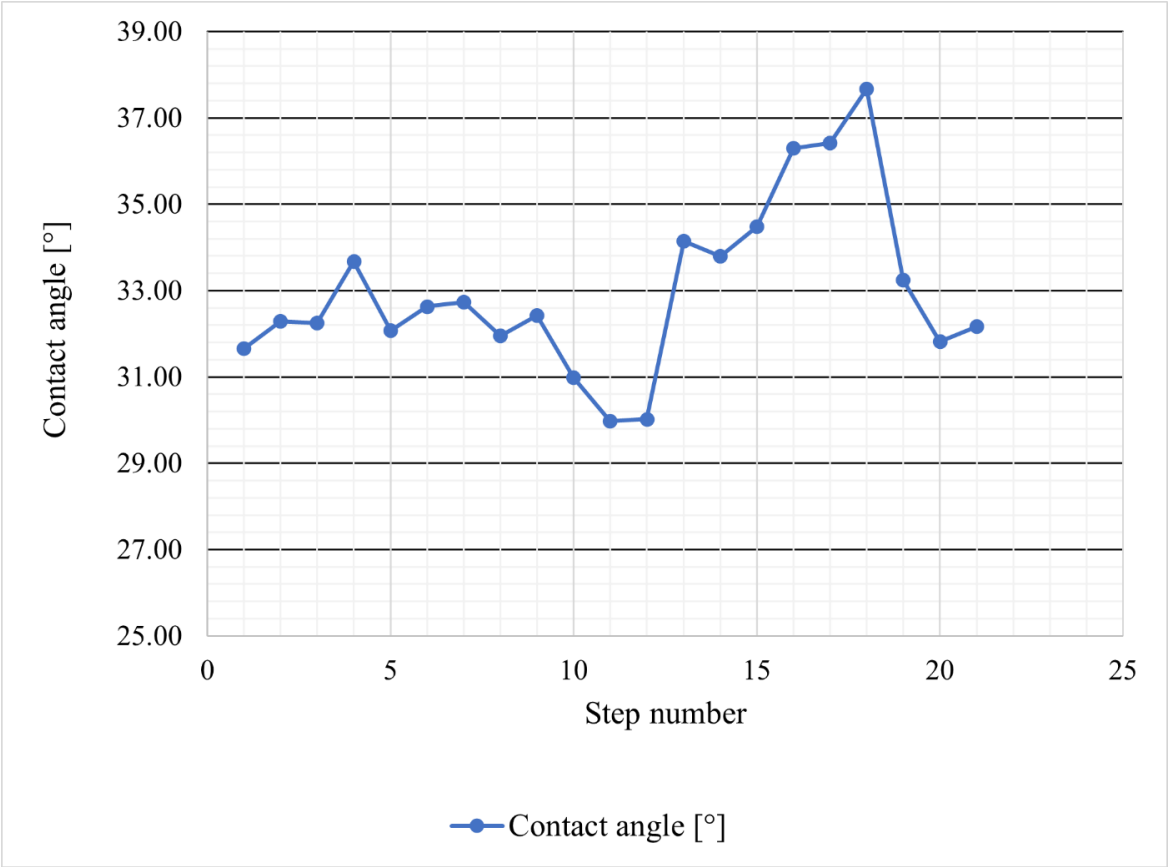

Figure 13. 21 Contact angle measurements carried out for neat epoxy blend using DSA 100.

Similarly, the nano-modified polymer blend was tested for contact angle measurements. The total measurements taken were 25 at the same room temperature, 20°C. The mean and standard deviations of these measurements are summarised in Table 3. The measurements are plotted in Figure 14. In contrast, the nano-modified polymer blend shows a higher contact angle of 60.13°. This suggests that the droplet on this film has less wetting or less interaction with the surface in comparison with the neat epoxy blend. Thus, the addition of A-GNPs has decreased the wettability of the film.

Table 3. Contact angle measurements of the nano-modified polymer blend

Parameters	Value	Standard Deviation
Mean diameter [mm]	2.39	0.05
Mean volume [µL]	1.69	0.10
Mean contact angle [°]	60.13	1.98

Table 4. Contact angle measurement test results for neat epoxy blend and nano-modified polymer blend

Sample	Mean Contact Angle [°]	Standard Deviation [°]
The neat Epoxy polymer film	32.98	1.98
Nano-indented polymer film	60.13	1.98

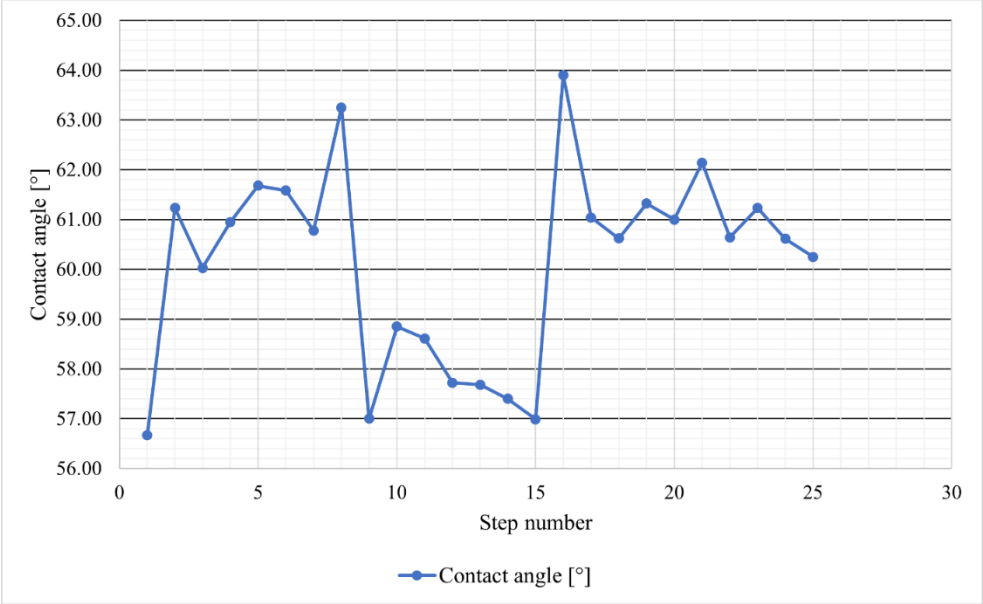

Figure 14. 25 contact angle measurements were carried out for the nano-modified polymer blend using DSA 100.

Table 4 provides comparative data on the contact angles and their variabilities for the neat polymer blend and nano-modified polymer film, offering insights into their wettability characteristics.

4.3 Summary

The results obtained demonstrated variations in Young's modulus and contact angles when comparing the two films, emphasizing the influence of A-GNPs on the material properties. Specifically, Young's modulus exhibited an increase upon the addition of A-GNPs in the hardener solution, up to a weight percentage of 50%. However, owing to the limited number of unique microstructures (only 5), applying DL techniques for predicting Young's modulus becomes unfeasible.

Regarding the contact angle measurements, the inclusion of A-GNPs led to a decrease in wettability for the composition. Notably, this property exhibited two distinct microstructures that either improved or reduced the wettability. Given that skilled personnel can easily test and evaluate this property, there is no necessity for DL in this scenario. The experimental method carried out by skilled individuals is sufficient for investing time and ensuring quality control as compared to DL methods.

The microstructure images collected during the blend fabrication can serve as a dataset. The DL applications to this dataset and its methodology are described in Chapter 5.

CHAPTER 5. DEEP LEARNING METHODOLOGY

In this chapter, the focus is placed on DL methodology applied to the nano-modified polymer composite. This will cover the data collection, DL model selection, and DL model design and development as shown in Figure 15. The testing stage will be discussed in the subsequent chapter (Chapter 6).

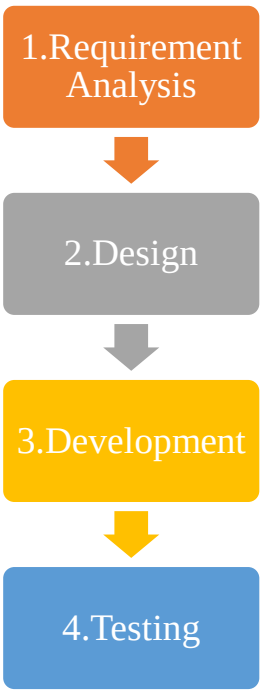

Figure 15. Software development life cycle

The first phase of the deep learning project involved a comprehensive Requirement Analysis. Based on the Requirement Analysis, the scope of the project was delineated, encompassing key considerations such as the type of deep learning model to be employed, be it classification, regression, or another paradigm. Identification of requisite data sources and establishment of performance metrics and success criteria were also integral components of this phase.

Following the Requirement Analysis, the Design phase was undertaken meticulously to plan the architecture of the deep learning model. This stage entailed critical decisions regarding the selection of appropriate deep learning frameworks, such as TensorFlow or PyTorch, and the programming language to be employed. The neural network architecture was designed, specifying the number of layers, types of layers, and activation functions. Additionally, data preparation

procedures, encompassing data cleaning, preprocessing, and partitioning into distinct training and testing sets, were delineated. Crucial hyperparameters, including learning rate, batch size, and regularization techniques, were also determined during this phase.

Subsequently, the Development phase was initiated, involving the actual implementation of the deep learning model and its supporting codebase. This stage saw the realization of the neural network architecture as per the design specifications. An intricate data pipeline was constructed to facilitate the loading, preprocessing, and augmentation of the data. The training loop, encompassing forward and backward passes, gradient descent, and weight updates, was meticulously coded. Additionally, evaluation and testing procedures were implemented to comprehensively assess the model's performance.

The final phase, Testing, constituted a critical evaluation of the deep learning model's performance and robustness. Rigorous testing procedures were executed to ascertain its ability to generalize effectively to unseen data, mitigating overfitting concerns. Comprehensive evaluation metrics, such as accuracy, precision, and recall, were employed to quantitatively gauge the model's performance. This phase culminated in a comprehensive validation of the model's efficacy and readiness for subsequent deployment.

5.1 Data collection

From past research and experiments conducted in Chapter 3, the property, and microstructural data were collected. Initially, 36 microstructure images were obtained from the previous researcher, of which 12 images were repeated (*i.e.* a total of 24 unique microstructure images). Three samples of nano-modified polymer composite had been tested for Young’s modulus and the images and corresponding property data were available.

As the data were limited in size further investigations on the property measurement were carried out for the remaining 8 samples mentioned in the methods section.

5.2 Formulating the problem statement

From the microstructure data and the properties of the nano-modified polymer nanocomposite, it is observed that the bi-continuous phase-separated microstructure with graphene-rich domains has shown a 97% increase in Young's modulus and 72% increase in thermal conductivity [3]. These properties suggest that this material is suitable for aerospace, automotive, and electronics applications. Therefore, the relationship between microstructure and property is important to study to understand this material so that other possible PNCs can be selected which show similar microstructure and diversify the selection set of suitable materials. Hence, the more suitable area for studying this PNC using DL techniques is identifying its favourable microstructure that results in these strong properties and identifying it from the set of given microstructure images using the image-based DL model. This fulfils the second research aim of this study.

5.3 Deep Learning Model Design

In the present case, the model should be able to distinguish a particular microstructure from the given set of images. The images are categorized into two groups 1. Phase separated (distinction of black and white regions) and 2. Homogeneous (dispersed regions). Hence, a CNN model is constructed for the binary image classification problem.

The architecture of the model is shown in below Figure 16.

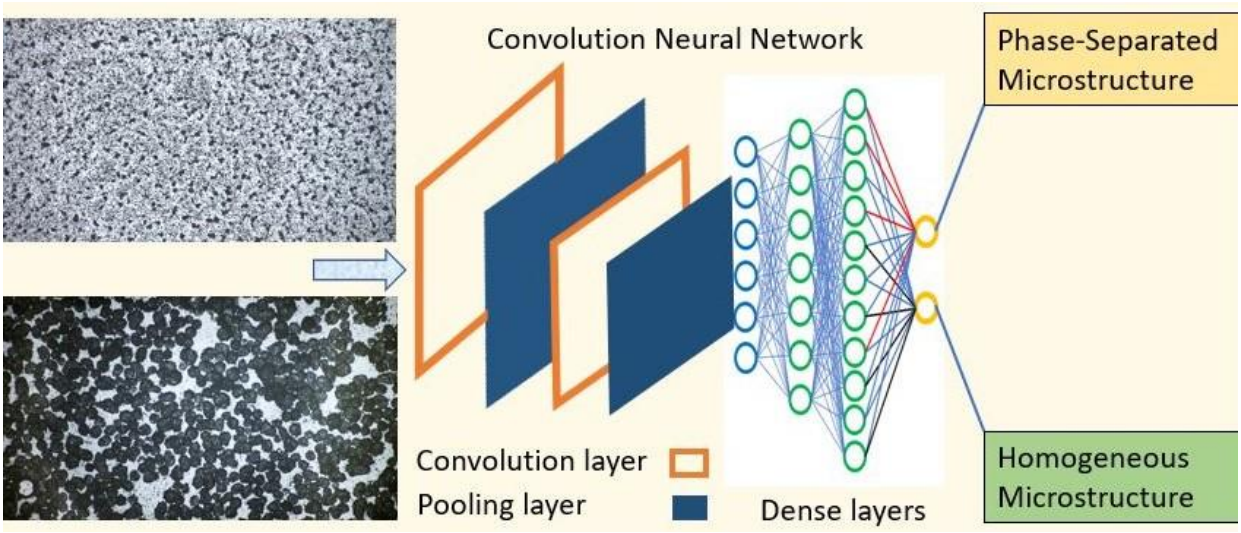

Figure 16. Schematic showing the Architecture of the CNN model.

Convolutional layers extract the information in terms of pixel values at given locations from image data and keep the extracted salient features intact. The image consists of a matrix of pixel values. The pixel is the smallest square in an image hence we can say that image is made up of these pixels. Every pixel has one value that shows the colour intensity, *e.g.* in an 8-bit grayscale image the pixel value can range between 0-255. For example, Figure 17. below shows what the pixels look like in the microstructure images. In CNN the convolution layers extract the patterns *e.g.* edges or circles from the given image by moving a kernel filter which is a small matrix passed on the whole image to scan the pixel values in the given image and then the feature map is generated by averaging the pixel values collected by convolutional layer. In some cases, padding is useful to retain the information from losing out due to inconsistency in the size of the feature map. Padding is a strategy utilized to maintain the spatial dimensions of the input image after convolution operations are performed on a feature map. It entails the addition of supplementary pixels surrounding the borders of the input feature map before the convolution process. Hence, this preserves the border information in an image.

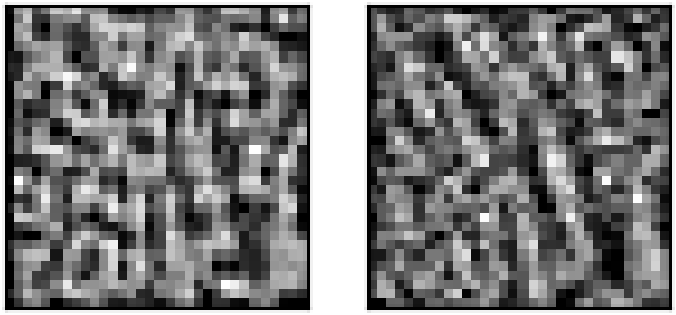

Figure 17. Pixels in a microstructure image

As realistic data do not always have linear dependencies, activation functions need to be added to the feature map to account for nonlinearity. As the name suggests, in the pooling operation the values generated by the feature map are maximized or averaged. As fully connected layers require dimension reduction of the incoming data, the pooling layer decreases the size of the feature map through the pooling operation. An important difference between CNN architecture and other DL architecture is that CNN uses hidden layers composed of convolutional, pooling or fully connected layers that follow each other [30]. Different CNN architectures utilize varying combinations of

convolutional and pooling layers. For example, the kernel filters and one output of the Conv2D layer are shown in Figure 17 and Figure 18 respectively.

For specific tasks such as classification or regression, fully connected layers are added to train on the extracted features from the image [31].

5.4 Model development

5.4.1 Data processing

The dimensions of all images were maintained uniformly (Width*Height) *i.e.*, 231*174 pixels, and stored in the. PNG format. To increase the dataset, an image augmentation technique was used. Data Augmentation is a widely employed technique in machine learning and DL that artificially expands the size of the training dataset [100]. It entails implementing diverse transformations or modifications on existing data samples, resulting in the generation of new and slightly altered versions of the original data. For the image data, the following transformations were used: Random cropping and resizing, Horizontal or vertical flipping, Rotation or shearing, Colour jittering or brightness adjustments, and Adding noise or blurring [101]. Data augmentation aims to enhance the generalization ability and robustness of machine learning models by testing them on a broader array of data variations and patterns. An example of the augmented image is shown in Figure 18. The displayed image has been generated utilizing seven operations mentioned below. No fill mode has been applied, resulting in default black edges. Since the image is produced by the data augmentation algorithm, the scale is unknown hence the scale bar cannot be shown. Due to such varied data, the model becomes more capable of handling different scenarios and improving its performance on unseen data. For the given dataset these operations were performed uniformly on every image using the ImageDataGenerator class from TensorFlow.

The details of the following operations are as below:

1. Rotation range in degrees = 90
2. Width_shift_range = 0.2
3. Height_shift_range = 0.2
4. Shear_range = 0.2
5. Zoom_range = 0.2

6. Vertical flipping
7. Horizontal flipping.
8. fill_mode = “reflect”

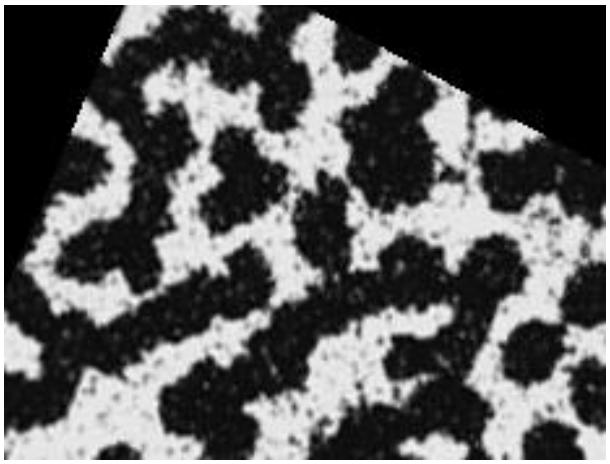

Figure 18. Microstructure image generated automatically using the data augmentation algorithm with parameters mentioned in Section 5.4.1 (scale unknown).

5.4.2 Code implementation:

The code was implemented using the TensorFlow and Keras [102] libraries in Python[1] in a Jupyter notebook[2]. The network architecture consisted of multiple layers, each with a specific function. The first layer of the network was a Conv2D layer with 32 filters, a kernel size of (3,3), and a ReLU [103] activation function. ReLU introduces non-linearity to the network, allowing CNNs to learn complex patterns and make non-linear transformations of the input data. It selectively activates neurons individually rather than all at once, and it transforms any negative value to zero as the output of the neuron. This makes the ReLU function computationally efficient and reduces overfitting [104].

[1] http://www.python.org
[2] (https://jupyter.org/in)

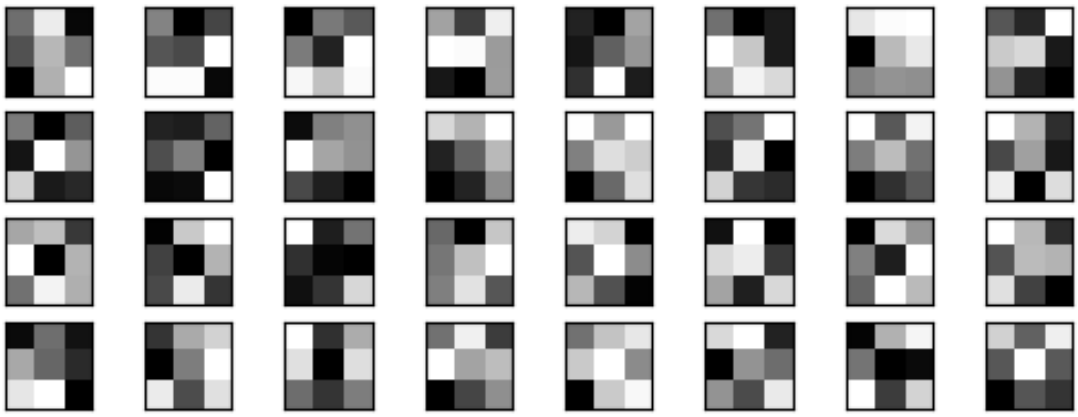

Figure 19. Kernal filters

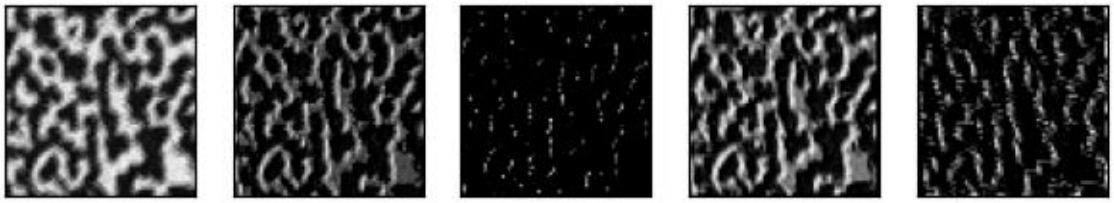

Figure 20. Convolution filter applied to a phase-separated microstructure.

The kernel size corresponds to the dimensions of the filter mask, denoted as width x height. Padding was set to 'same', meaning the spatial dimensions of the input and output will be the same. The output of this layer was then passed to a MaxPooling2D layer with a pool size of (2,2). This layer reduced the spatial dimensions of the feature maps to prevent overfitting. The output of the pooling layer was then normalized using a BatchNormalization layer with axis=-1, which normalized the activations of the preceding layer. A Dropout layer with a rate of 0.2 was then applied, randomly setting 20% of the input units to 0 during training, helping to prevent overfitting. The output of the Dropout layer was then flattened into a 1D vector and passed to a fully connected Dense layer with 512 units and a ReLU activation function. The final layer was another Dense layer with 2 units and a sigmoidal activation function, representing the binary classification output.

The model was compiled with the Adam optimizer [105], a categorical cross-entropy loss function, and accuracy as the evaluation metric. Adam optimizer computes the loss function at each step and adjusts the learning rate hence it is an adaptive learning rate as compared to Gradient descent where the learning rate is constant. At the end of the output layer, the Sigmoid activation function is used which converts the output in terms of 0 or 1 based on probability score.

The sigmoidal function is defined as:

$$F(x)=\frac{1}{1+e^{-x}} \qquad \text{Equation 2}$$

In this equation, "e" represents the base of the natural logarithm, and "x" is the input value to the sigmoid function. The function takes the input value "x" and applies a mathematical transformation to it, resulting in an output value between 0 and 1.

The sigmoidal function has an "S"-shaped curve and is shown in the Figure. 21[3] below, starting from 0 as "x" approaches negative infinity, and gradually increasing towards 1 as "x" approaches positive infinity. The midpoint of the sigmoid curve, where the output is 0.5, occurs at "x = 0". The function is commonly used in logistic regression models to predict binary outcomes, where the output indicates the probability with which it belongs to that specific class. It squashes the input values to a probability range, making it useful for classification tasks.

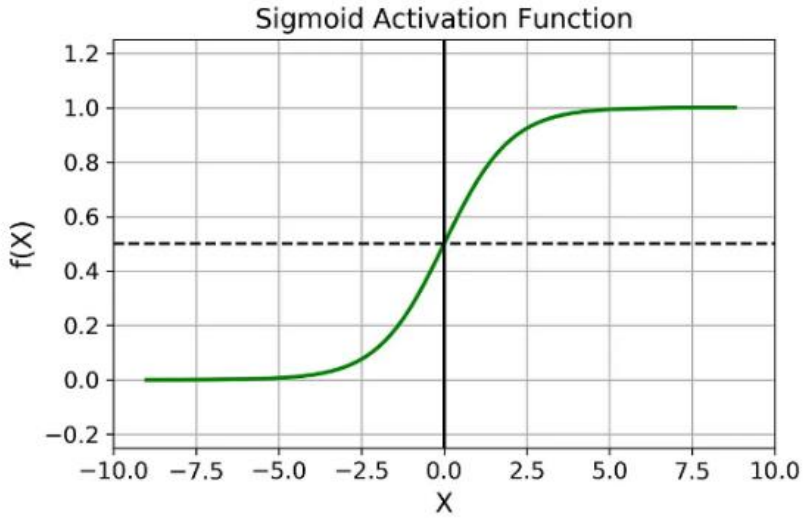

Figure21. Sigmoidal activation function (source: https://medium.com/analytics-vidhya/activation-functions-all-you-need-to-know-355a850d025e)

The dataset was partitioned into train and test sets by performing an 80/20 split, with labels encoded as categorical variables. The model underwent 20 epochs of training using a batch size of 20. These hyperparameters are finalised after checking the effect of these parameters on the accuracy of the model. A few initial iterations are shown in Figures 22 and 23 respectively.

[3] https://medium.com/analytics-vidhya/activation-functions-all-you-need-to-know-355a850d025e

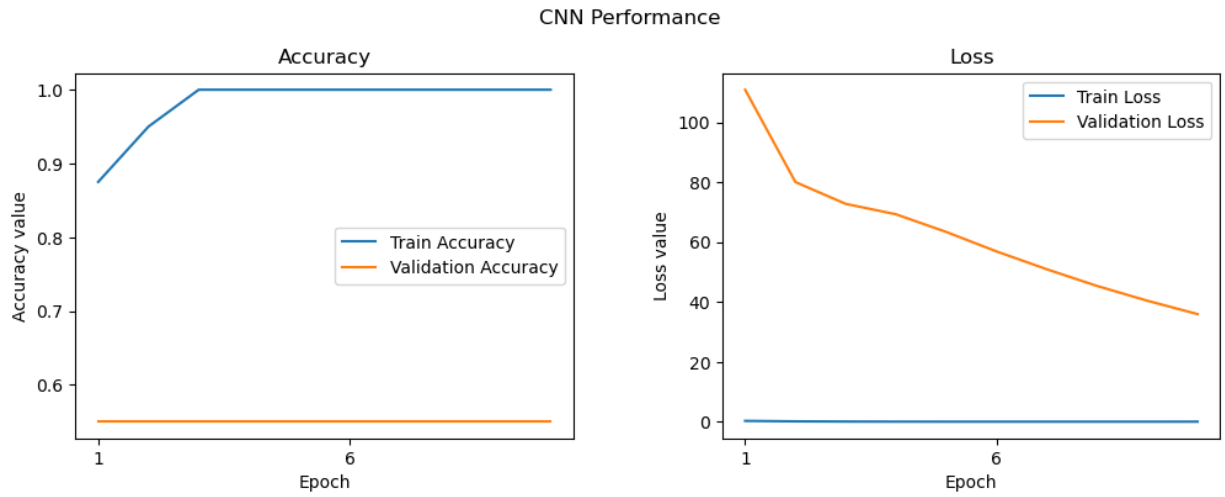

Figure 21. Accuracy and Loss after the first iteration.

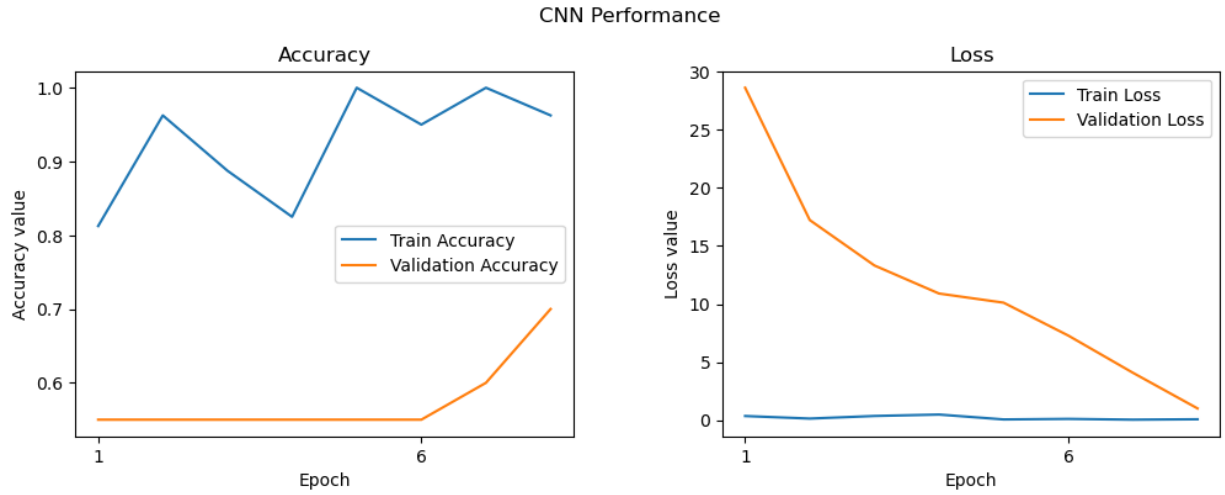

Figure 22. Accuracy and loss after the second iteration.

One commonly used metric which assesses the learning of a CNN model from the training data is accuracy and training loss. The training dataset, which is a subset of the overall dataset, is used to initially train the model, while the validation dataset, another subset of the data, is reserved to validate the model's performance.

The accuracy is determined by the ratio of predicted values (ypred) that match with actual values (ytrue) to the total predicted values. If the predicted label of the microstructure image (phase separated or homogeneous) matches the true label, it is considered accurate. The training accuracy of the training data is given as the deviation of the predicted value from the actual value for the training dataset. The training loss is determined by adding the errors for each training set example.

After each epoch, the validation loss is determined by adding the errors for each sample in the validation set. An epoch refers to one complete iteration of processing the entire training set by the model, and the training loss is determined after each batch. The “number of epochs,” an important hyperparameter, must be set while training the model, determining how many times the learning algorithm will process the whole training dataset. This allows for determining whether the model requires additional learning or hyperparameter tuning.

The Training Accuracy curve exhibits a discernible upward trajectory, indicating a progressive improvement in the model's proficiency in classifying samples from the training set. In contrast, the Validation Accuracy curve remains notably flat, suggesting a lack of substantial improvement in accuracy on the validation set across epochs. This conspicuous gap between the two curves raises concerns regarding potential overfitting. Overfitting is a phenomenon wherein the model becomes excessively specialized in fitting to the nuances and noise of the training data, potentially compromising its ability to generalize to new, unseen samples.

The Validation Loss curve delineates the loss on a separate validation data set that remains unseen by the model during the training process. This validation set serves as a litmus test for the model's ability to generalize to new, unseen data. In the present analysis, a noteworthy observation emerges from the validation loss curve: it showcases a decreasing trend, albeit with a substantial gap for the the training loss curve. This disparity between the validation and training loss curves raises an important consideration. A notable divergence between the two curves may be indicative of overfitting and consequence, the model's performance on new, unseen data may be compromised.

In conclusion, while the current performance of the CNN classification model provides valuable insights, it also highlights avenues for refinement and enhancement. The dropout technique is already implemented but still further options needs be explored to enhance the model's generalization capacity. Furthermore, considerations for acquiring additional data and optimizing model complexity warrant close attention. The steps taken to optimise the performance and the benchmarking it with the literature is discussed in the next chapter, *i.e.* Chapter 6.

In summary, the code is given in Figure 22. builds and trains a CNN for binary image classification using the Keras library in Python. The model parameters are summarised in Table 5. The total time required for the tuning and training was 2 days on a general laptop. In this case, DELL latitude 5421 with core i7 was used for training and testing of the model.

Table 5. Summary of the parameters used to develop the CNN architecture.

	Parameter	Selected value or option
Model specification	Optimizer	Adam
	Body Activation	ReLU (Rectified Linear Unit)
	Output Activation	Sigmoid
Compilation	Loss	Binary cross entropy
	Optimizer	Adam
	Metric	accuracy
Validation	Training data	80%
	Testing data	20%
	Batch size	5

5.4 Summary

In this chapter, the initial three stages of the software development lifecycle were successfully executed, which encompassed use case analysis of requirements, design, and development. The first stage involved collecting data and finalizing the use case based on the gathered information. In the design stage, the layout for the CNN architecture was carefully planned out. Subsequently, in the development stage, the CNN model was implemented by writing code in Jupyter Notebook. The code for the developed model is available on GitHub[4] for easy access and reference. This model will be tested on the mixed microstructure images of novel nano-modified polymer composite. The process of training and testing of the DL model is thoroughly discussed in the Chapter 6.

Some of the code implementation is shown in Figure 24 given below:

[4] https://github.com/Anuradhamk/MScR/blob/main/Phase_classification_cnn-1.py

```
flat=keras.layers.Flatten()(drop2)
```

```
hidden1=keras.layers.Dense(512,activation='relu')(flat)
norm3=keras.layers.BatchNormalization(axis=-1)(hidden1)
drop3=keras.layers.Dropout(rate=0.2)(norm3)
```

```
conv1=keras.layers.Conv2D(32,kernel_size=(3,3),
                          activation='relu',
                          padding='same')(inp)
```

```
pool1=keras.layers.MaxPooling2D(pool_size=(2,2))(conv1)
norm1=keras.layers.BatchNormalization(axis=-1)(pool1)
drop1=keras.layers.Dropout(rate=0.2)(norm1)
```

```
out=keras.layers.Dense(2,activation='sigmoid')(drop4)
```

```
model=keras.Model(inputs=inp,outputs=out)
```

```
model.compile(optimizer='adam',
              loss='binary_crossentropy',
              metrics=['accuracy'])
```

Figure 23. Code used to operate the CNN model.

CHAPTER 6: TESTING AND RESULTS

This chapter assesses the performance of DL using various performance metrics. To determine how well the algorithm was efficient to distinguish between phase-separated and homogeneous samples, the model was assessed by Accuracy metrics[5] from Keras DL library. The second metric used in addition to the Accuracy metric is by plotting the confusion matrix.

6.1 Testing on the old dataset

The accuracy plot (Figure 25(a)) reveals that in this initial study, the trained accuracy is 95%, but the validation accuracy of the CNN model was found to be 65.4%. This means that when the model is tested on the training dataset, 95% of the images were tested accurately but when the trained model is used on the 20% of test images to which the model had not previously been exposed, the model correctly identified only 65.4% of these test images. Similarly, the training loss on the training data was 0.18 compared with a validation loss of 2.6 on the validation dataset. The model's performance on training and validation data is shown in terms of accuracy and loss in Figures 23a and b, respectively.

The first plot, which displays the relationship between the accuracy value and the epoch, highlights the distinction between the validation accuracy curve and the train accuracy curve. This indicates that the training data are insufficient in number, as the validation accuracy does not converge to the values of the training accuracy. This suggests that the data in the validation set are new to the model and have not been seen before, hence the predictions made are largely inaccurate. This is an important factor since it represents the generalizability of the model, *i.e.* how well a model can fit the new unseen data. To increase the generalizability of the model it is important to achieve the same accuracy for the training dataset and validation dataset. Graphically the training accuracy and validation accuracy curves should converge. As seen from the second plot (b) the training loss and validation loss curves are converging. This alone does not guarantee the performance of the

[5] https://keras.io/api/metrics/accuracy_metrics/

model.

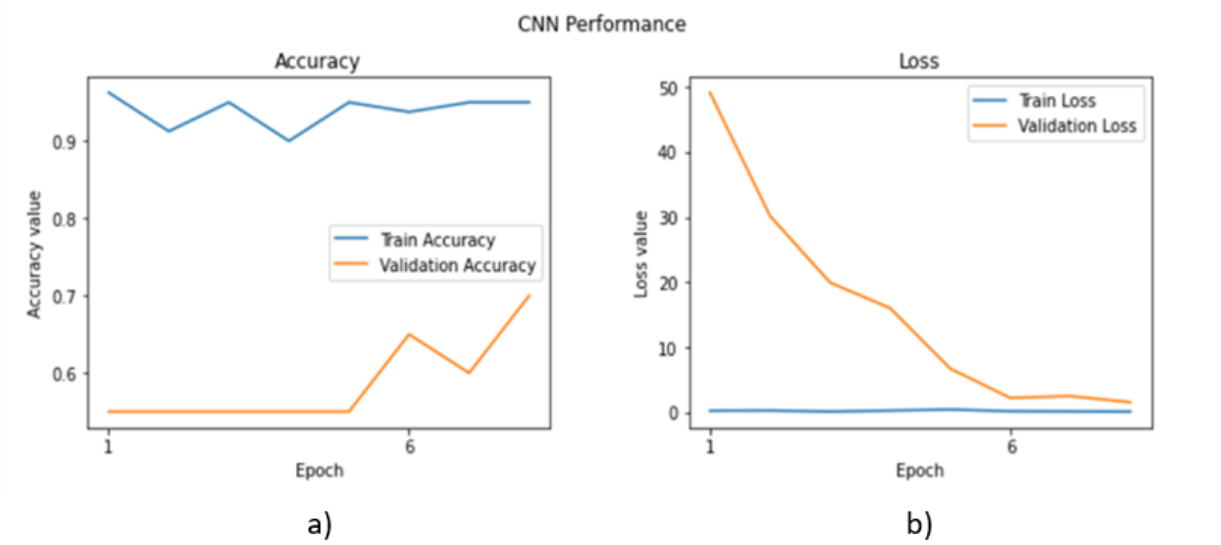

Figure 24. Evaluation of the performance of the CNN as a function of (a) Training accuracy *versus* test accuracy and (b) Training loss and validation loss for the Stage 1 dataset.

The Confusion Matrix [106], which is shown in Figure 26, is plotted to assess the model's predictions in detail. The matrix compares the predicted labels of the images by the model (on the X-axis) with the true labels of the images (on the Y-axis). The four cells in the matrix used in this evaluation are: True positive (when the model correctly identifies a phase-separated microstructure, shown in the bottom right corner of the matrix), False positive (when the model mistakenly identifies a homogeneous microstructure as phase separated, shown in the top right cell), True negative (when the model correctly identifies a homogeneous microstructure, shown in the bottom left cell), and False negative (when the model mistakenly identifies a phase-separated microstructure as homogeneous, shown in the top left corner). Based on Figure 26, it is evident that the model incorrectly categorized 12 images of homogeneous microstructures as phase-separated microstructures. To illustrate this, an example of one image has been included that falls under the 'False Positive' category. Additionally, the figure displays examples of the 'True Positive' and 'True Negative' categories, which depict the actual images classified by the mode in these categories.

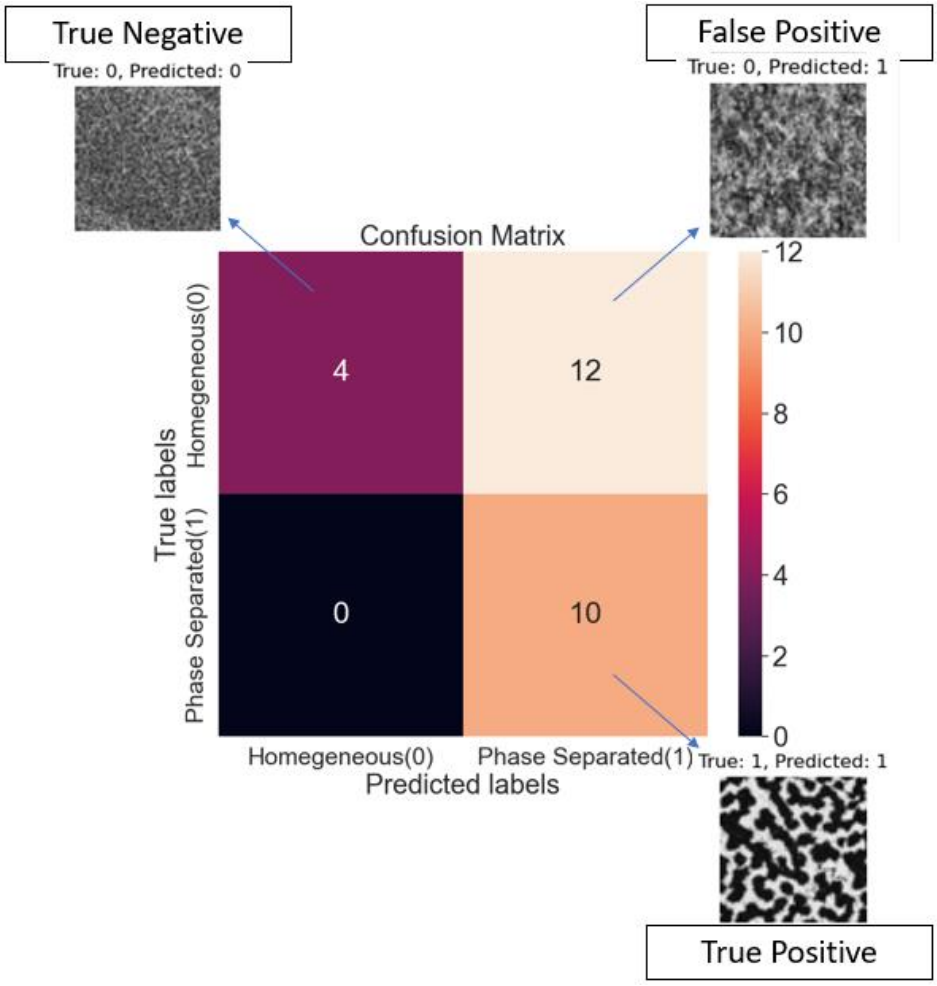

Figure 25. Confusion matrix for stage 1 dataset

Furthermore, the F1 score [107] is calculated using the True positive, False positive, and False negative values to trade-off between the precision and recall using the formulae listed below in Equations 3, 4, and 5, respectively [32]. The precision score and recall score metrics are calculated to understand the true influence of the True positive using the following formulae. Precision and recall are measures of a model's accuracy, where precision evaluates the accuracy of positive predictions made by the model while recall assesses the model's capability to identify all positive instances. A high precision score indicates that the model makes few minimal false positive predictions, meaning it correctly predicts positive only for instances that are truly positive. A high recall score signifies that the model is capable of accurately identifying a majority of the positive instances. The F1 score balances the trade-off between precision and recall, serving as an overall measure of a model's accuracy.

$$\text{Precision} = \frac{\text{True positive}}{\text{Actual Result (True positive + False positive)}} \quad \text{Equation 3}$$

$$\text{Recall} = \frac{\text{True positive}}{\text{Predicted Result (True positive + False negative)}} \quad \text{Equation 4}$$

$$\text{F1 score} = \frac{2*\text{precision}*\text{recall}}{\text{precision} + \text{recall}} \quad \text{Equation 5}$$

The precision score is 0.7 and the recall score is 0.6. Overall, the F1 score obtained for this model is 0.5, where the higher the F1 score the better the model's ability to predict accurately. Thus, the current F1 score needs improvement.

6.2 Feedback and corrective measures

Additionally, previous studies using DL methods have also assessed the model's performance by measuring the accuracy and loss, thus Azimi *et al.* reported achieving 93.94% classification accuracy for steel microstructure classification using DL methods and obtaining an accuracy of 48.89% surpassing the state-of-the-art approach significantly [33]. Chowdhury *et al.* reported a case study on dendritic morphologies using the pre-trained neural networks for two micrograph classification tasks and achieved accuracies up to 91.85 and 97.37, respectively [34]. A general and transferable deep learning (GTDL) framework built to predict phase formation in materials was able to discriminate five types of phases with accuracy and recall more than 94% [35]. The F1 score used in a previous study to classify the microstructure of titanium, steel, and powder using convolutional neural networks obtained an F1 score of 0.8 [32]. Based on the above assessments of the model using accuracy metrics, the confusion matrix, and the F1 score, along with relevant literature, it has been determined that the original dataset should be expanded by conducting additional experiments and adding more original images to train the model.

To increase the original image dataset, experiments were repeated to fabricate the new films by following the same steps mentioned in Section 3.1 of Chapter 3. However, the data acquisition and microstructure characterization methods were changed due to the laboratory conditions and availability of equipment.

6.2.1 Data Generation

The current setup had limited data acquisition capabilities. To address this, Professor Jonathan Howse from the Department of Chemical and Biological Engineering at the University of Sheffield provided access to advanced data acquisition equipment and various microscopes for conducting experiments and acquiring data. These experiments focused on film fabrication using diverse methods including blade-spreading as shown in figure 27, coverslip and slide quenching as shown in figure 28, and spin coating as shown in figure 29 respectively. Additionally, the nano-modified blends were subjected to curing at various temperatures such as 50°C, 21°C, and corresponding microstructure evaluation was observed using an optical microscope equipped with a data acquisition system. This allowed for the examination of the influence of curing temperatures on the microstructure. The impact of different blend fabrication methods on their microstructures was assessed by studying these structures after curing at varying temperatures and utilizing data acquisition techniques.

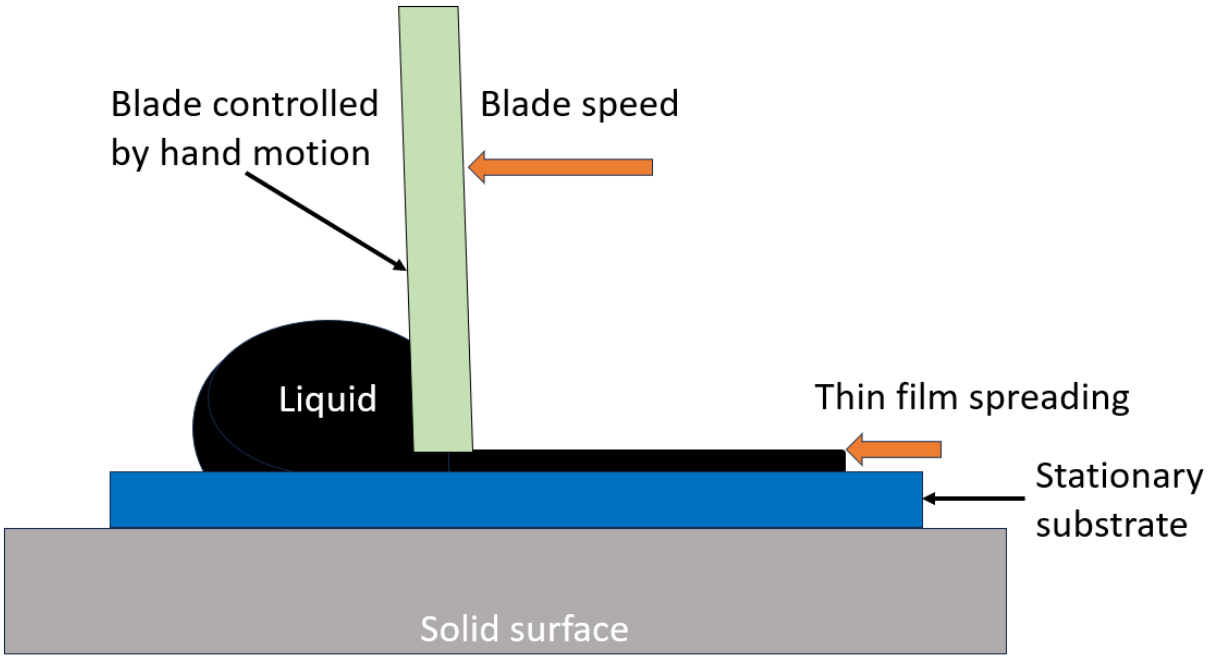

Figure 26. Schematic of blade-spreading method used for nano-modified thin film fabrication

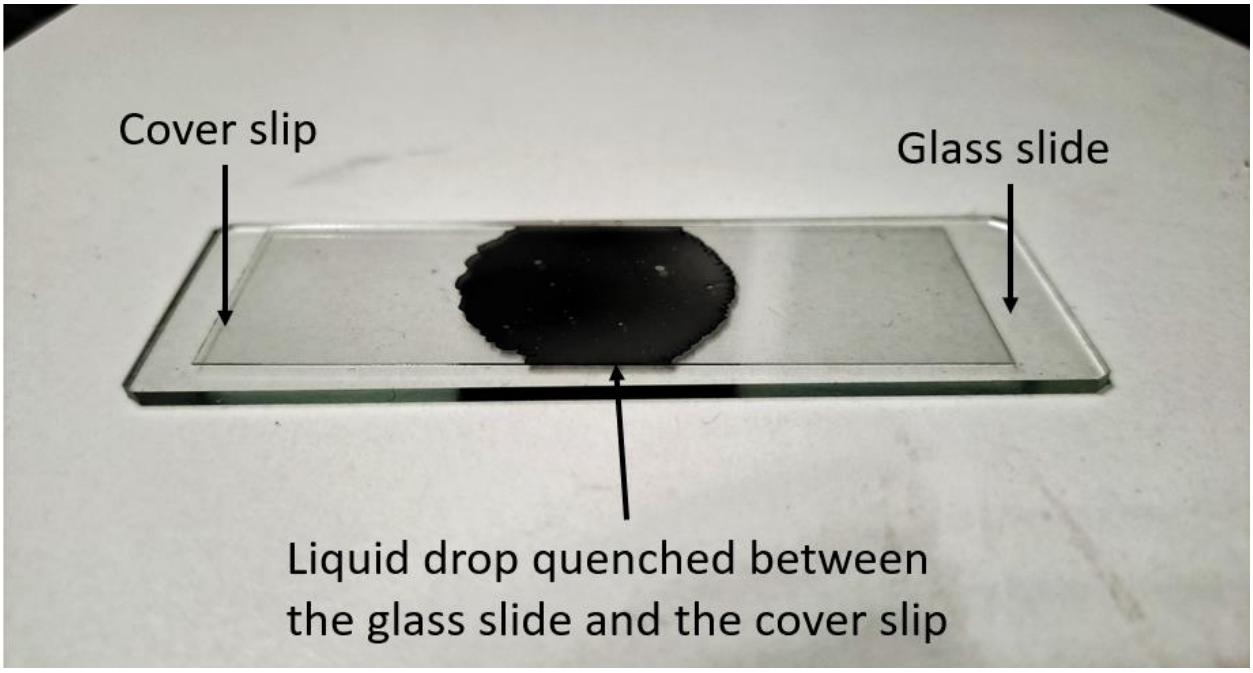

Figure 27. Contact slip and Slide quenching method where a liquid droplet of nano-modified polymer blend is quenched between a contact slip and a glass slide.

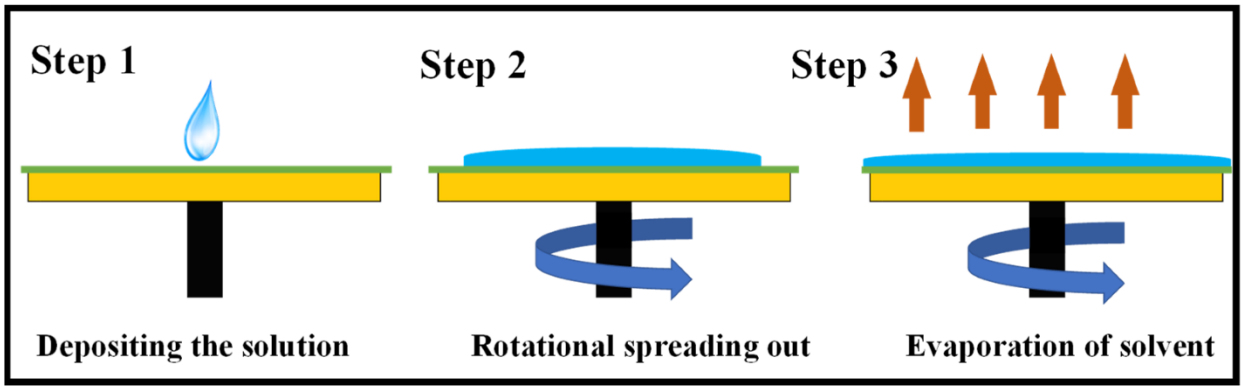

Figure 28. Stages of spin-coating of thin-film on a substrate. Step 1: Solution is deposited on the substrate. Step 2: Rotational spread out of the solution. Step 3: Evaporation of the solvent, image used with permission from [108].

In the blade-spreading method, manual movement of the blade over the liquid introduced uneven force due to potential human error. Consequently, this led to inconsistent film thickness, making it challenging to achieve uniformity when fabricating blends of the same thickness. In contrast, the coverslip and slide quenching method reduced the spatial movement of particles in the droplet,

resulting in a lower dispersion compared to spin coating, where centrifugal force aided in mobilizing the particles within the liquid. The primary objective was to achieve a range of microstructures, both phase-separated and homogeneous, while maintaining consistent film thickness. Ultimately, spin coating consistently yielded similar results across repeated experiments, making it the standard method for blend fabrication.

The experiment setup is shown in Figure 30. The microstructure image acquisition of the spun-coated films was performed through a bespoke experiment . The spun coated film on a glass slide is immediately placed on the Peltier element (SP1848-27145 TEC1 Thermoelectric Heatsink Cooler Peltier Plate Module) which was maintained at 50◦C using a DC power supply from Tenma Model 72-8345A Switching Mode Bench at 4.7 V and 0.53 A of current. The voltage and current settings to maintain the 50°C were calibrated before the experiments. The calibration setup is shown in Figure 28 along with the temperature gradient of the Peltier module in Table 6.

The heatsink placed below the Peltier element prevented the overheating by dissipating the heat to the surrounding surface and air. The silicon wafer with aluminium coating was used to keep the surface beneath the sample clean and shiny so that the reflection of the light from the microscope noise proof. The microstructure was observed to examine the dispersion of A-GNPs within the epoxy matrix using the Nikon objective lens of 10x magnification power. The complete setup with data acquisition is shown in Figure 32.

Figure 29. Experimental setup for Peltier module calibration

Table 6. Calibration of Peltier module.

Current (Amp)	Voltage (V)	Temperature (deg)	Time (min)
0.55	4.2	47	0
0.53	4.7	63	10
0.53	4.7	65.5	20
0.58	5.2	71	30
0.63	5.7	75.5	40
0.66	6.2	82	50
0.7	6.7	87	60

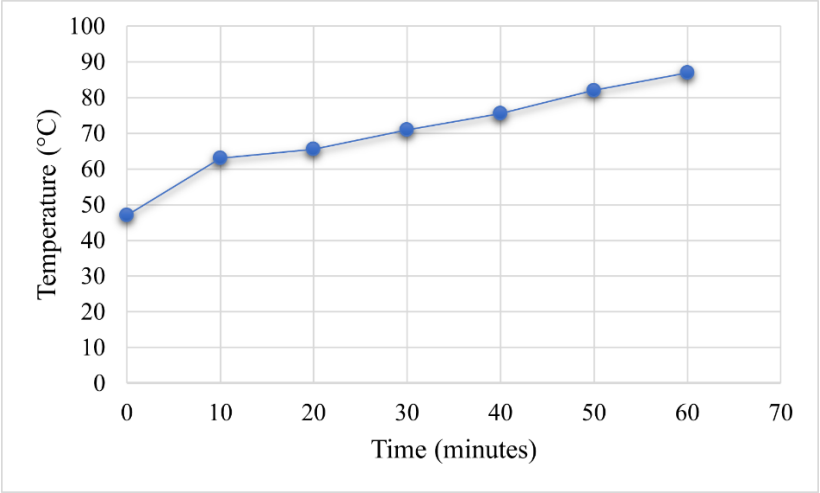

Figure 30. The temperature gradient of the Peltier module.

6.2.2 Data Acquisition

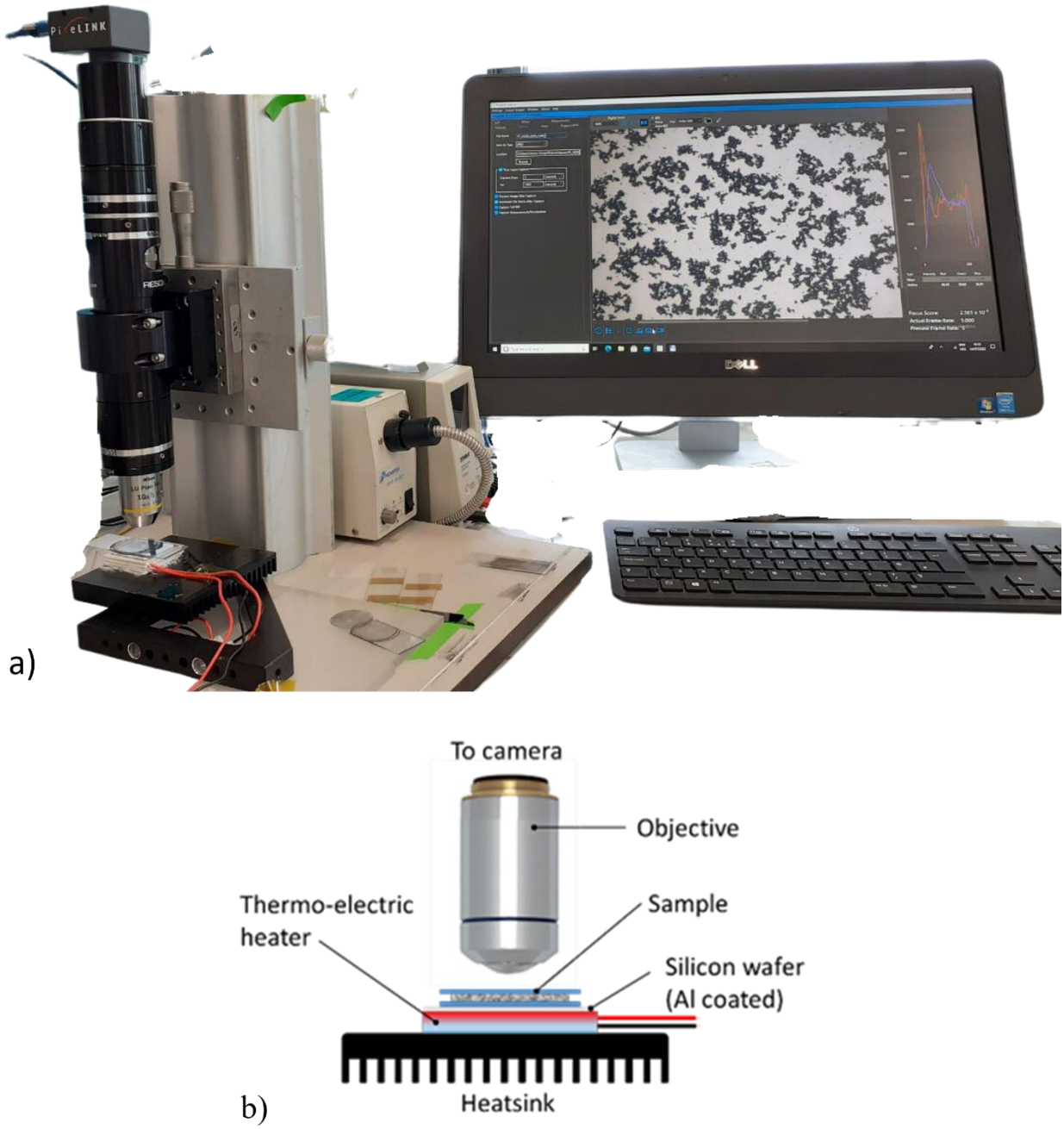

Figure 31. a) *In-situ* data acquisition setup at the University of Sheffield, b) Schematic representation of the setup

The Pixelink camera module (Pixelink PL-D7718CU-T, 1/2.3", 18MP, C-Mount USB 3.0 Colour Camera) was attached to the Nikon objective lens and the microstructure images were acquired using Pixelink Capture software. These images were captured at a frame rate of 1fps with 5.8 ms

exposure time and saved in .jpg format in the selected directory. Using this set up the data acquisition was carried out over 10 minutes per film to ensure that the microstructure construction is fully completed (this typically occurs during the initial 6–8 mins). After that, the spun-coated film is placed into an oven for 5 hrs. The final cured microstructure was captured to verify the change in morphology during the oven heating.

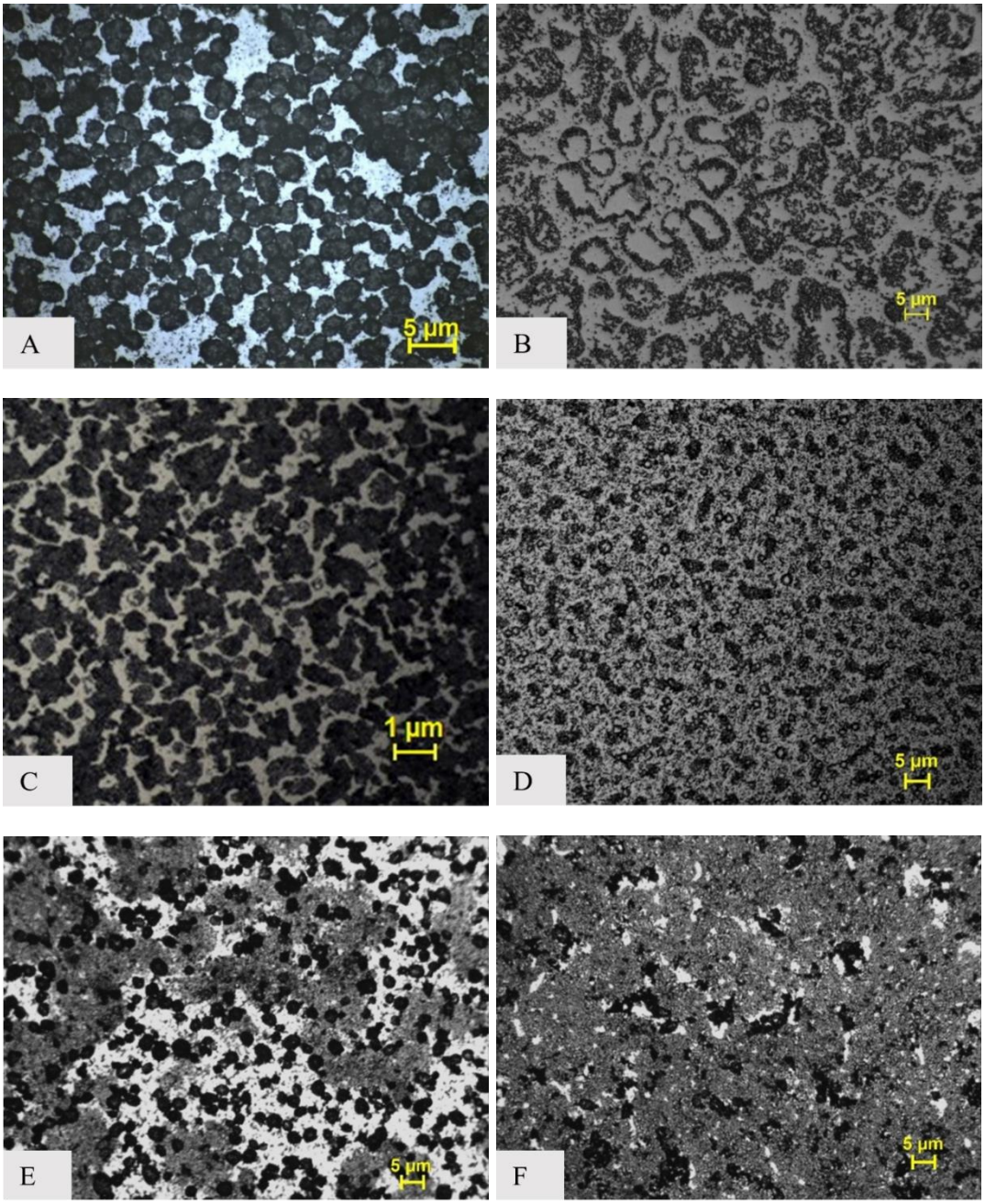

Figure 32Images captured using optical microscope showcasing various microstructures of novel nano-modified polymer composite films produced with Epoxy Resin, MH 137, and A-GNPs at

the University of Sheffield. (a-c) Depict a phase-separated microstructure featuring distinct graphene domains achieved with 3 weight % of A-GNPs in the total blend. (d-f) Exhibit a homogeneous microstructure of the blend with varying weight percentages of A-GNPs.

The phase-separated microstructure occurs when the reaction pairs begin to undergo crosslinking, and are thus prone to separate away from unreacted pairs to form two distinct phases from the miscible blend during the polymerization (shown in Figure 33 a), b), c) which represents examples of the new data set acquired. The second type of microstructure with homogeneously dispersed A-GNPs is abbreviated as a homogeneous microstructure (where the A-GNP is homogeneously dispersed in epoxy resin) as shown in Figure 33. d), e) and f).

6.3 Testing on the Newly generated dataset

The newly expanded dataset consisted of 350 images after incorporating newly obtained images from the second set of experiments. This dataset was then used to train the previously constructed CNN model for identifying the microstructure of phase-separated polymers while keeping the same values for the hyperparameters *i.e.* batch size, number of epochs, and validation data split. The model is first assessed by the accuracy metric displayed in Figure 34 a) and b), respectively. In this plot the validation accuracy and train accuracy curves converge closely with a validation accuracy of 80.1%, significantly greater than the previous case based on a limited dataset, while the validation loss and training loss also converged to a much lower value of 0.6 as shown in Figure 34 a) and b), respectively.

Additionally, the model was evaluated using a confusion matrix, a common technique in classification problems. In this case, the extended dataset provided a diverse collection of microstructural images, which leads to a larger training data set. This enhances the model's ability to learn and recognize the unique spatial features present in both phase-separated and homogeneous microstructure images and therefore correctly identify the structured extreme dark and white regions in phase-separated microstructure. However, this is limited particularly in situations where the blend has only just begun to disperse. As illustrated in Figure 35, the model incorrectly classified three images of homogeneous microstructures as phase separated, even though small dark regions were only just beginning to appear in the white regions, indicating dispersion, which was classified as 'False Positive' according to the Confusion Matrix. To provide an example of this, an image has been included that the model categorized within this grouping.

The precision, recall, and F1 score were calculated for this model, and these are 0.94, 0.91, and 0.92, respectively.

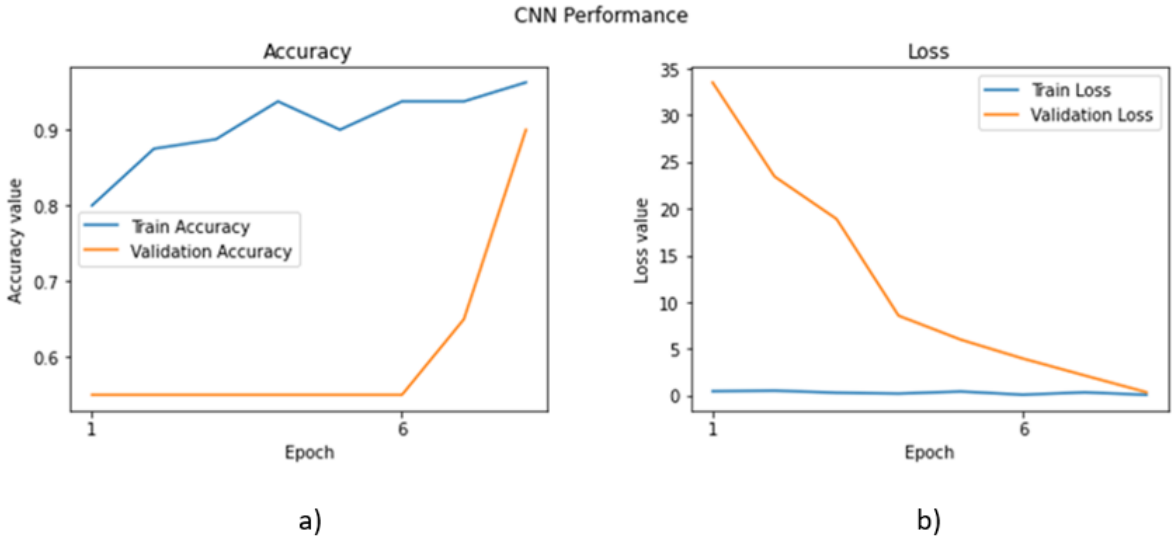

Figure 33. Performance of the CNN as a function of (a) Training accuracy versus test accuracy and (b) Training loss and validation loss for the extended dataset

6.4 Summary

In this chapter, the final stage of the software development life cycle is executed. The model that was developed and described in Chapter 5 is now subjected to testing using the old dataset. Two metrics, namely Accuracy and Confusion Matrix, are utilized for the testing process. The initial test results are carefully examined which showed the poor accuracy of model in microstructure classification task. Data scrutiny and literature comparisons lead to the generation of corrective measures. From finding it was concluded that the current dataset needs to be expanded further. As part of the expansion of the original dataset, new experiments are conducted. From these newly generated datasets, the model could learn from a wider variety of data. The second stage dataset is then subjected to testing using the same metrics employed earlier. The results demonstrate a noticeable improvement compared to the initial testing phase. A detailed discussion surrounding this outcome is presented in the subsequent chapter, Chapter 7.

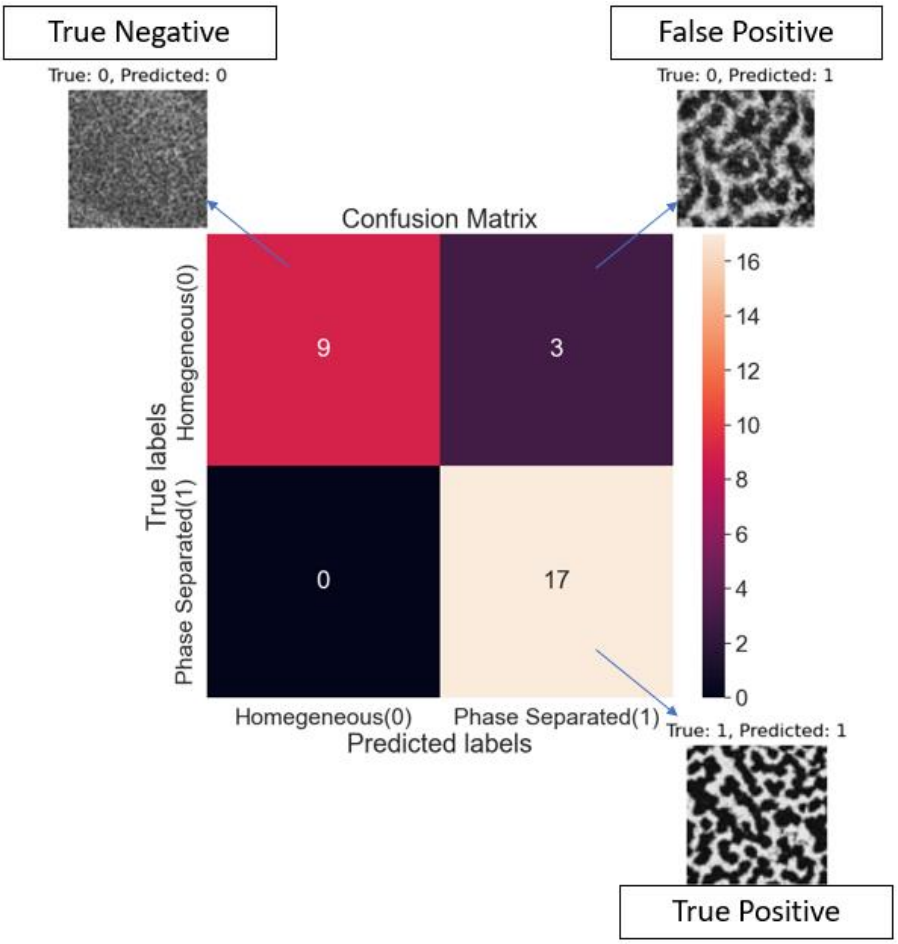

Figure 34. Confusion matrix for extended (stage 2) dataset

CHAPTER 7. DISCUSSION

This chapter will cover the overall discussion surrounding experiments and DL tools. In this chapter the previously developed DL model will be used on a new dataset to find out whether DL can perform better and if it is suitable for phase separation identification problems.

7.1 Experimental methods and results:

Firstly, the literature review highlighted the potential of DL techniques for studying the microstructure of complex materials such as polymer nanocomposites. These methods offer advantages in analysing large datasets and identifying intricate relationships within composite components. It was observed that the novel nano-modified polymer composite, with its exceptional mechanical and thermal properties, held promise for applications in electronics coatings. However, further research was warranted to understand the microstructure of this new composite fully. The utilization of data-driven methods, including DL, proved to be efficient and cost-effective compared to traditional experimental characterization and simulation methods. This underscored the importance of validating DL methods for studying newly developed polymer nanocomposites, fulfilling the first research aim.

The summary of the chemical composition and processing parameters for nano-modified polymer composite are mentioned in Figure 36 and Table 7 respectively.

Regarding Young's Modulus, an increase was observed with the addition of A-GNPs in the hardener solution, up to a weight percentage of 50%. However, the limited number of unique microstructures (only five) posed challenges when applying DL techniques for predicting Young's Modulus. The complexity and variability of the microstructures necessitate a larger and more diverse dataset for accurate predictions, rendering DL unfeasible in this particular case.

In terms of contact angle measurements, the inclusion of A-GNPs resulted in reduced wettability of the composite. Notably, two distinct microstructures were identified, each either improving or reducing the wettability. Given that skilled personnel can effectively test and evaluate this property, the use of DL is deemed unnecessary.

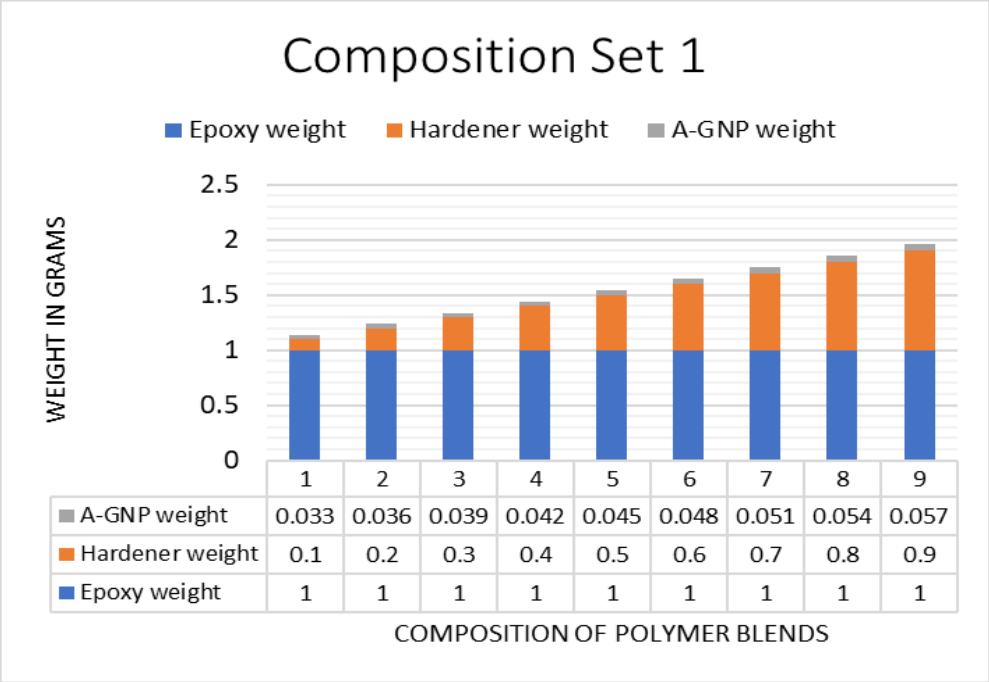

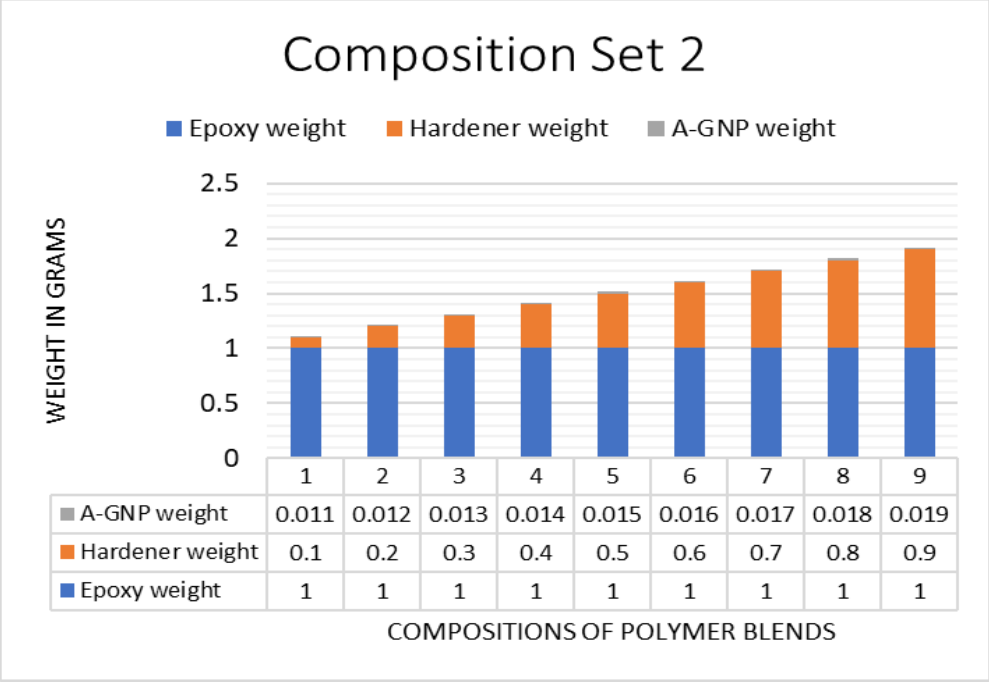

Figure 35. Summary of the chemical compositions of the polymer blend and A-GNP.

Table 7. Summary of the experimental observations

Room temperature (°C)	24.2
Spin coating time (min.)	1
Spin coating speed (RPM)	1500
Dispersion time (min.)	180
Curing temperature (°C)	50
Curing time (min.)	300

7.2 Deep Learning Method

For microstructural studies, convolutional neural networks (CNNs) emerged as a suitable DL model. CNNs have predominant applications in computer vision for image recognition tasks, effectively extracting features from images, making them ideal for analysing microstructural patterns. The choice of CNN as the DL model aligned with the research objective of distinguishing between phase-separated self-assembled microstructures reinforced with graphene domains and homogeneous microstructures.

Lastly, to identify how accurately the model can work as a classifier, the ROC curve is plotted. To plot the ROC curve, the true positive rate is plotted on the y-axis and the false positive rate on the

y-axis. To construct a ROC curve, the classification model's output, often a probability score or a continuous prediction, is used to rank the instances. The threshold is then applied to determine the predicted class labels. By varying the threshold from high to low, different points on the ROC curve are obtained. At each threshold, the true positive rate (TPR) is calculated as the ratio of accurately predicted positive instances to all real positive instances. The false positive rate (FPR) is determined by the ratio of inaccurately predicted positive instances to the overall number of true negative instances. An ideal classifier should have a TPR of 1 and an FPR of 0, indicating perfect classification. In such a case, the ROC curve would pass through the top-left corner of the plot. Conversely, a random classifier would exhibit a ROC curve that closely mimics a diagonal line with a positive gradient *i.e.* from the plot’s bottom left to its top right.

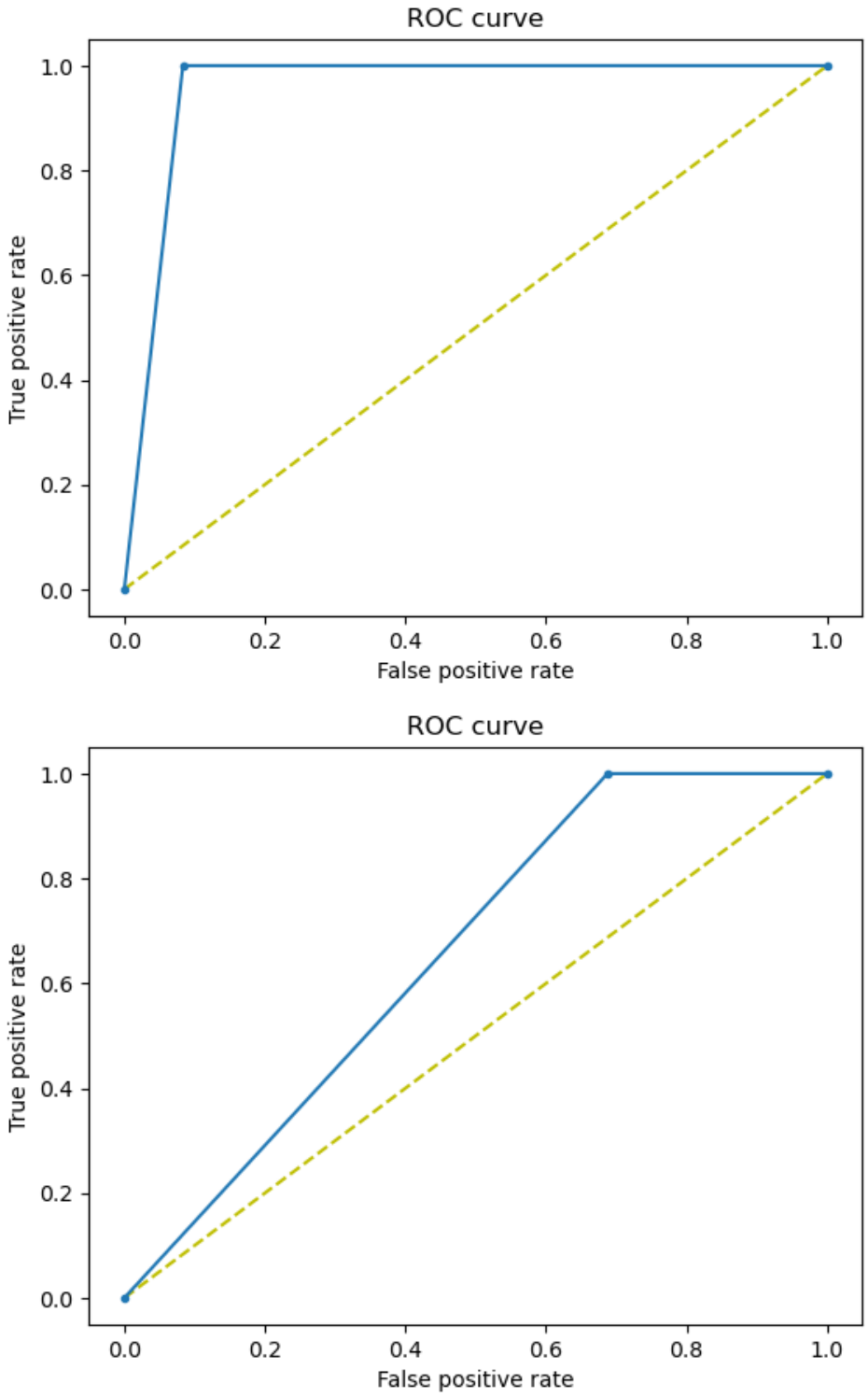

Figure 36. Receiver Operating Characteristic (ROC) curve of CNN classification model trained on (a) Stage 1 dataset and (b) Extended dataset

The ROC curve provides a visual representation of the model's discriminatory power or its ability to distinguish between positive and negative instances. A model's performance is considered better when the ROC curve is positioned closer to the top-left corner. The area under the ROC curve (AUC – ROC) can be used as a quantitative metric to assess the model's performance. A perfect classifier is indicated by an AUC – ROC value of 1, whereas a random classifier is represented by an AUC – ROC value of 0.5.

The ROC curve and the associated AUC-ROC analysis are widely used in ML and evaluation of classification models, particularly in medical diagnostics, fraud detection, and many other domains where the balance between true positive and false positive rates is crucial. Furthermore, to evaluate the FPR and TPR of the classifier model, the ROC curve was plotted for both cases (a) the Stage 1 dataset and b) the extended dataset, as depicted in Figure 37 a) and b), respectively. The left curve was obtained from the earlier model trained on a limited dataset and the right one with an improved ROC curve was obtained after the dataset had been expanded. The actual classification result is also shown in Figure 38 and Figure 39 for stage 1 dataset and stage 2 dataset. From the comparison, the latter shows significantly improved predictions and hence it is now a reliable classifier model. Hence this updated model satisfies the third research aim of the thesis.

The testing results of the DL model demonstrated the iterative nature of the software development life cycle. The initial testing phase highlighted areas requiring improvement, leading to corrective measures such as data generated through experiments. The second stage dataset was then tested using the same metrics employed in the initial testing, revealing substantial improvement compared to the previous phase. These results underscored the importance of continuous evaluation, refinement, and optimization in DL models.

The automated screening of microstructure can process a high volume of images saving lots of time and ensuring the quality of screening. For the more complex problem such as predicting chemical composition from microstructure or processing history, the ground truth data must be large *e.g.* at least 1000 images of microstructures including all range of variations of microstructure for the change in composition. Some of the researchers have used the simulation methods to generate the images instead of experiments in that case simulation method may not depict the experimental result due to boundary conditions set in the simulation as well as experimental

constraints. The skilled personnel in the material science domain needs to complement the person who is developing the data-driven model.

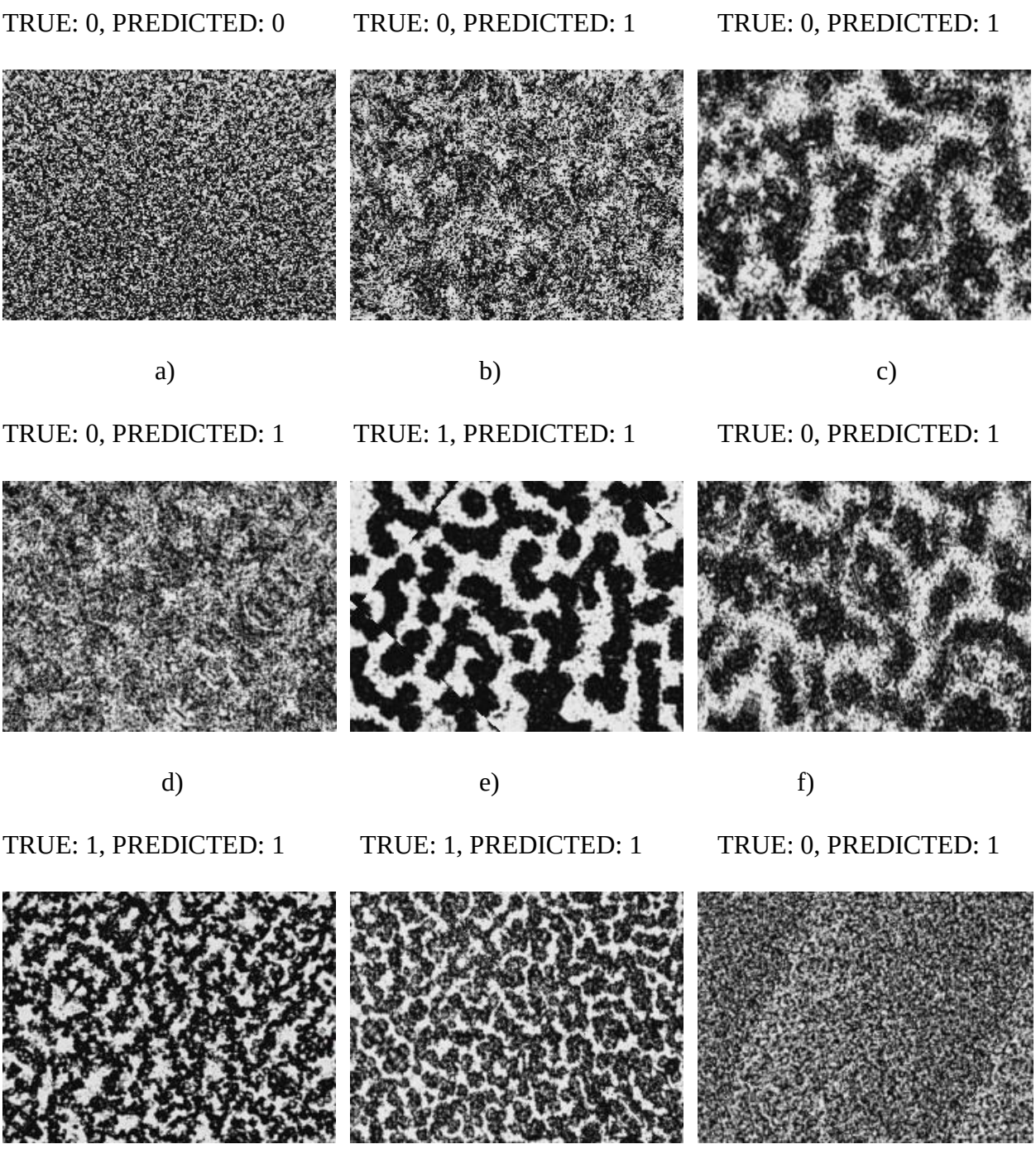

Figure 37. Classification result on stage 1 dataset.

TRUE: 1, PREDICTED: 1 TRUE: 1, PREDICTED: 1 TRUE: 1, PREDICTED: 1

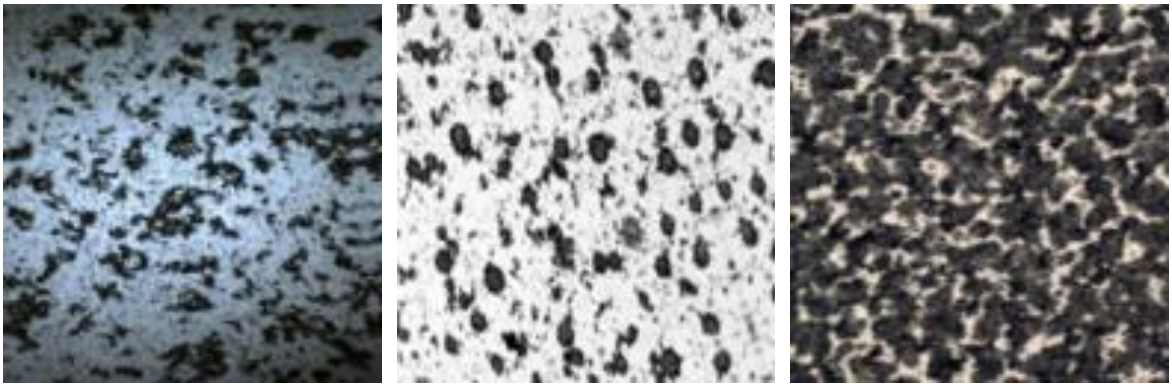

a) b) c)

TRUE: 1, PREDICTED: 1 TRUE: 1, PREDICTED: 1 TRUE: 1, PREDICTED: 1

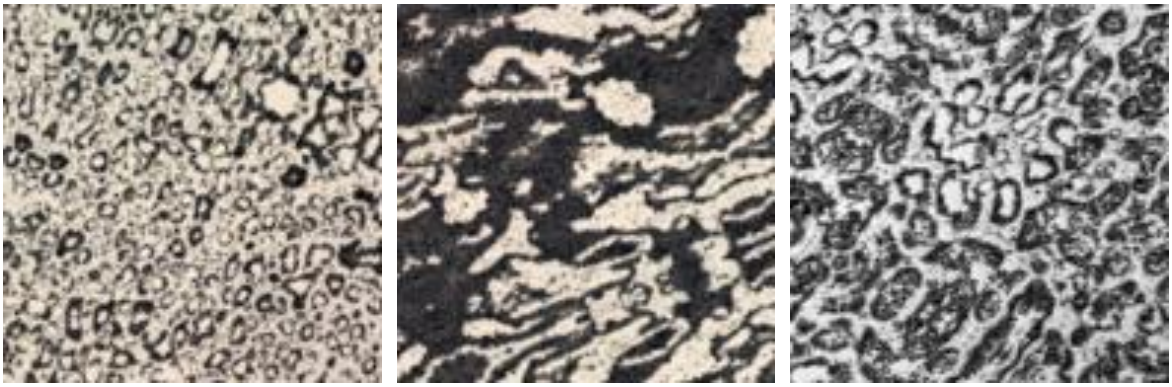

d) e) f)

TRUE:0, PREDICTED: 0 TRUE: 0, PREDICTED: 0 TRUE: 0, PREDICTED: 0

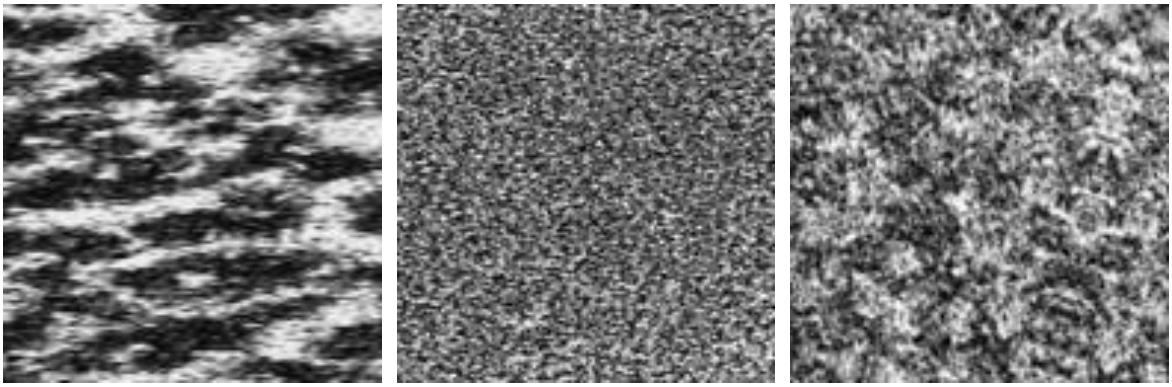

g) h) i)

Figure 38. Classification result on stage 2 dataset

CHAPTER 8. CONCLUSIONS AND FUTURE SCOPE

8.1 Conclusions

The research question posed in this thesis, "Can we use DL techniques to identify the development of phase behaviour in a novel nano-modified polymer composite?", aimed to explore the potential application of DL in studying the microstructure and phase behaviour of complex materials. The objectives were successfully achieved through a comprehensive literature review, the development of a DL model, and the testing of the model on relevant datasets. The literature review highlighted the potential of DL techniques in analysing large amounts of data and identifying complex relationships in polymer nanocomposites and CNN was the majorly used artificial neural net. The novel nano-modified polymer composite, with its exceptional mechanical and thermal properties, presented an ideal candidate for DL-based analysis.

The experimental results, including the determination of Young's modulus and contact angle measurements, provided insights into the material properties and the influence of A-GNPs on these properties. The findings were discussed comprehensively, emphasizing the importance of skilled personnel in evaluating certain properties, such as wettability, without the need for DL methods.

The DL model, specifically the CNN architecture, was successfully designed and developed based on the identified research aims and objectives. The model showed promising results in distinguishing between different microstructures in epoxy blends, achieving an accuracy of 80.8% and an F1 score of 0.92 for categorizing phase-separated self-assembled microstructures and homogeneous microstructures. The ROC curve indicated that the model closely resembled a perfect classifier when tested on an expanded dataset. This research demonstrates the potential of data-driven methods for analysing polymer nanocomposites, offering a more efficient alternative to traditional characterization techniques such as AFM, which are costly and time-consuming. This finding fulfils the second research aim of this study. The findings suggest that these methods can have a significant impact on studying phase-separated microstructures, potentially facilitating inverse design by predicting the required composition for phase separation. This could save considerable time and effort compared to relying solely on experimental methods. By utilizing

CNNs in DL, this study effectively identified the desired microstructure of a novel nano-modified polymer composite known for its exceptional properties.

In conclusion, this research demonstrates the potential of DL techniques, particularly CNN, in studying the microstructure and phase behaviour of novel nano-modified polymer composites. The developed DL model successfully distinguished between different microstructures, offering an efficient alternative to traditional characterization techniques. The findings contribute to the advancement of data-driven methods in polymer nanocomposite research and lay the foundation for future applications of DL in predicting phase separation and understanding the influence of various parameters on microstructure formation. Further, currently available data can be used to train such models which can impact the advancement of innovations in material science. By adopting data-driven methods, the traditional approach of taking 5-10 years to develop a solution or product, from innovation to application in industry, can be significantly accelerated. Data-driven approaches facilitate faster discovery and can optimize the entire development process.

The challenges associated with the application of DL methods were identified, including the requirement for representative and sufficient training data, as well as the trade-off between data collection efforts and problem criticality. These challenges were addressed and discussed, providing insights into the limitations and considerations for potential applications of DL in similar research areas.

The challenges associated with the application of DL methods can be summarized as follows:

1. The effectiveness of the model in solving a given problem relies on whether the training data adequately represents the various variations and complexities present in the data. Additionally, the quantity of data available also plays a crucial role in the performance of the model.
2. When selecting a problem statement, it is essential to consider the trade-off between the resources required for data collection and the criticality of the problem at hand. In situations where extensive data collection is necessary, it is worth exploring alternative methods that can provide insights or solutions while considering the importance and urgency of the problem.

These remarks conclude the third research aim of this study.

8.2 Lessons learnt

Throughout this thesis, several valuable lessons have been acquired, which have enhanced our understanding of the application of DL techniques in studying novel nano-modified polymer composites. The following lessons summarize the key insights gained from this research endeavour:

8.2.1 Importance of Literature Review:

A comprehensive literature review played a pivotal role in this study, enabling us to grasp the existing knowledge landscape and identify research gaps. Through an in-depth analysis of previous works, we were able to discern the suitability of DL techniques for studying polymer nanocomposites and the potential benefits they offer in terms of analysing complex microstructures. This emphasized the importance of conducting a thorough literature review to inform and guide research directions.

8.2.2 Data Collection and Pre-processing Challenges:

The process of data collection for the novel nano-modified polymer composite presented certain challenges. Access to relevant and high-quality data proved to be a key concern, requiring careful selection and evaluation of available datasets. Additionally, data pre-processing tasks, including cleaning, normalization, and feature extraction, were essential to ensure the reliability and suitability of the data for DL analysis. The importance of addressing these challenges early on was crucial in establishing a solid foundation for subsequent modelling and analysis.

8.2.3 Model Development and Selection:

Developing an appropriate deep-learning model for studying the microstructure of the polymer composite was a critical aspect of this research. Informed by prior works that demonstrated the effectiveness of convolutional neural networks (CNNs) in image-related tasks, the CNN architecture was chosen as the most suitable model for this study. This selection process highlighted the significance of understanding the strengths and limitations of different DL models and aligning them with the research objectives.

8.2.4 Training and Testing:

The training and testing phases of the DL model provided valuable insights. The model's performance was influenced by various factors, including the selection of appropriate hyperparameters, the availability and diversity of training data, and the prevention of overfitting. Rigorous testing on unseen data was instrumental in assessing the model's accuracy, generalization capabilities, and potential for practical applications. The iterative refinement of the model based on testing results was a key lesson learned for achieving robust and reliable predictions.

8.2.5 Experimental Limitations:

This research encountered limitations in the experimental setup, notably the limited number of unique microstructures used in the study. Consequently, applying DL techniques for predicting Young's Modulus became unfeasible due to the insufficient variation in the data. This highlighted the need for expanding the dataset to encompass a broader range of microstructures in future research. Furthermore, considering alternative approaches or complementary methods to address the limitations of DL in certain scenarios should be explored.

6. Trade-off between Deep Learning and Traditional Methods:

A fundamental consideration arising from this study is the trade-off between the resources required for DL analysis and the criticality of the research problem. DL techniques, while powerful and efficient, necessitate substantial data collection efforts and computational resources. Therefore, it is essential to carefully evaluate the cost-effectiveness and importance of the research problem when deciding to employ DL or rely on traditional characterization techniques. A thoughtful assessment of the problem's complexity and urgency will guide researchers in selecting the most appropriate approach.

8.3 Future Outlook

The future scope of this research involves expanding the predictive capabilities of DL models to forecast phase separation in nanocomposites. The user, *e.g.* a researcher, will be entering the composition of different components and the model will be able to predict the microstructure and ultimately determine whether the given composition will lead to a favourable microstructure which

gives excellent properties, in this case, if it would be a phase-separated microstructure or homogeneous microstructure. This will greatly benefit researchers who currently rely on iterative experiments and characterization methods in the lab to innovate polymer nanocomposites. This saves resources required in laboratories such as consumables to conduct the experiments, reduces chemical waste and saves man hours. To achieve this, it is crucial to consider additional parameters, such as the Hildebrand solubility parameter, viscosity, and thermal properties, to enhance the model's understanding of how these factors influence the resulting microstructure. This will require careful consideration of input data structure, parameter tuning, training and thorough testing. The collection of data should be conducted meticulously with the guidance of domain experts, as it will serve as the foundation for the model's learning process.

This approach can not only be applied to the novel nano-modified polymer composite but also to identify optimal combinations of polymers and nanofillers. By understanding the phase separation phenomena, researchers can utilize this method to reverse-engineer the desired microstructure that aligns with specific application requirements. This approach takes into consideration the relationship between material properties and microstructure, enabling researchers to design and achieve the desired microstructure for a particular application.

In addition to this, researchers will be able to utilize automated classification models to swiftly scan vast databases of materials and identify favourable ones. This approach proves especially beneficial when dealing with immense volumes of data, where error-free results are crucial and must be obtained within minutes. One industry that can greatly benefit from such applications is the plastics recycling industry. Conventional methods for polymer sorting and separation face inherent limitations, especially when dealing with composite materials featuring intricate nanostructures. The manual and mechanical approaches currently employed struggle to discern the specific phases within these advanced materials [109]. However, with the advent of CNN models specialized for phase identification, a promising avenue emerges for precise categorization and separation. The CNN model, designed to discern nuanced structural features e.g. morphology, is uniquely poised to overcome this hurdle. The advanced model trained for phase identification and composition prediction paves the way for efficient recycling processes [110].

Moreover, the economic viability of employing such advanced technologies cannot be understated. While initial implementation may necessitate investment, the long-term gains in terms of

streamlined recycling operations and the recovery of high-value materials are anticipated to far outweigh the costs. As the plastic recycling industry continues to evolve, the integration of CNN models for classification of material based on it's microstructure or phase stands at the forefront of technological progress. It not only addresses existing challenges in recycling nano-modified polymer composites but also positions the industry on a trajectory toward greater sustainability and efficiency therefore showing the potential impact on the plastic recycling industry. This innovative approach heralds a new era in recycling technology, poised to play a pivotal role in shaping the future of the plastic recycling industry.

To enhance recycling efficiency in this field, companies are actively seeking techniques that can effectively categorize incoming plastic materials from primary sources. The primary focus lies in the recovery of pure forms of recycled poly(ethylene terephthalate) (PET), which has wide applications in the plastic industry *e.g.* plastic containers for food storage, thin film wrappers for food packaging and water bottles *etc*. It is essential to accurately identify and separate such materials from a given mixture of various materials. Currently, manual execution of this task requires significant effort and is prone to human errors, such as inaccuracies caused by employee fatigue. Alternatively, the characterisation methods based on infrared technologies are currently being investigated for this application, *etc*. These methods are efficient but are only suitable for low volume. In industry, the waste recovery process is in continuous operation thereby making these methods likely expensive and slow. However, by boosting these existing characterization techniques with AI algorithms based on image recognition, the developed infrastructure will be capable of scanning incoming materials, identifying them, and categorizing them correctly within minutes.

Furthermore, organizations dedicated to environmental engineering, such as "The Ocean Cleanup [6]" are actively progressing in the development of sophisticated technologies to understand the underlying mechanisms governing the behaviour of plastics in marine ecosystems. Their research extends to comprehending and detecting various polymer types and configurations, aiming for an efficient removal process from our oceans. The deep learning models formulated in this thesis have the potential to advance to the point of recognizing polymer types through image analysis and composition assessment, complementing sensor-based techniques. Given the escalating severity

[6] https://theoceancleanup.com/research/

of the climate crisis, it is imperative to seek collaborative solutions with environmental entities like The Ocean Cleanup to effectively mitigate its impact.

REFERENCES

[1] R. Hsissou, R. Seghiri, Z. Benzekri, M. Hilali, M. Rafik and A. Elharfi, Polymer composite materials: A comprehensive review, Composite Structures 2021, Volume 262, Pages 113640.

[2] H. Fischer, Polymer nanocomposites: from fundamental research to specific applications, Materials Science and Engineering: C 2003, Volume 23, Issue 6, Pages 763-772.

[3] S. He, H. Stadler, X. Huang, X. Zheng, G. Yuan, M. Kuball, M. Unger, C. Ward and I. Hamerton, Self-assembled microstructures with localized graphene domains in an epoxy blend and their related properties, Applied Surface Science 2023, Volume 607, Pages 154925.

[4] J. Njuguna and K. Pielichowski, Polymer nanocomposites for aerospace applications: properties, Advanced Engineering Materials 2003, Volume 5, Issue 11, Pages 769-778.

[5] M. Gong, L. Zhang and P. Wan, Polymer nanocomposite meshes for flexible electronic devices, Progress in Polymer Science 2020, Volume 107, Pages 101279.

[6] B. Fiedler, F.H. Gojny, M.H.G. Wichmann, M.C.M. Nolte and K. Schulte, Fundamental aspects of nano-reinforced composites, Composites Science and Technology 2006, Volume 66, Issue 16, Pages 3115-3125.

[7] D.G. Galpayage Dona, M. Wang, M. Liu, N. Motta, E. Waclawik and C. Yan, Recent advances in fabrication and characterization of graphene-polymer nanocomposites, Graphene 2012, Volume 1, Issue 2, Pages 30-49.

[8] K. Hu, D.D. Kulkarni, I. Choi and V.V. Tsukruk, Graphene-polymer nanocomposites for structural and functional applications, Progress in Polymer Science 2014, Volume 39, Issue 11, Pages 1934-1972.

[9] Z. Sekhavat Pour and M. Ghaemy, Polymer grafted graphene oxide: For improved dispersion in epoxy resin and enhancement of mechanical properties of nanocomposite, Composites Science and Technology 2016, Volume 136, Pages 145-157.

[10] Z.P. Luo and J.H. Koo, Quantification of the layer dispersion degree in polymer layered silicate nanocomposites by transmission electron microscopy, Polymer 2008, Volume 49, Issue 7, Pages 1841-1852.

[11] D. Ciprari, K. Jacob and R. Tannenbaum, Characterization of polymer nanocomposite interphase and its impact on mechanical properties, Macromolecules 2006, Volume 39, Issue 19, Pages 6565-6573.

[12] M.A. Bashir, Use of dynamic mechanical analysis (DMA) for characterizing interfacial interactions in filled polymers, Solids 2021, Volume 2, Issue 1, Pages 108-120.
[13] L. Shen, T. Liu, and C. He, Nanoindentation and morphological studies of epoxy nanocomposites, Macromolecular Materials and Engineering 2006, Volume 291, Pages 1358-1366.
[14] J. Zhao, L. Wu, C. Zhan, Q. Shao, Z. Guo and L. Zhang, Overview of polymer nanocomposites: Computer simulation understanding of physical properties, Polymer 2017, Volume 133, Pages 272-287.
[15] A. Karatrantos, N. Clarke and M. Kröger, Modeling of polymer structure and conformations in polymer nanocomposites from atomistic to mesoscale: a review, Polymer Reviews 2016, Volume 56, Issue 3, Pages 385-428.
[16] S. Guryel, M. Walker, P. Geerlings, F. De Proft and M.R. Wilson, Molecular dynamics simulations of the structure and the morphology of graphene/polymer nanocomposites, Physical Chemistry Chemical Physics, 2017, Volume 19, Issue 20, Pages 12959-12969.
[17] J. Liu, Y.Y. Gao, D.P. Cao, L.Q. Zhang and Z.H. Guo, Nanoparticle dispersion and aggregation in polymer nanocomposites: insights from molecular dynamics simulation, Langmuir 2011, Volume 27, Issue 12, Pages 7926-7933.
[18] S. Yu, S. Yang and M. Cho, Multi-scale modelling of cross-linked epoxy nanocomposites, Polymer 2009, Volume 50, Issue 3, Pages 945-952.
[19] J.D. Durrant and J.A. McCammon, Molecular dynamics simulations and drug discovery, BMC Biology, 2011 Volume 9, Issue 1, Pages 71.
[20] S.A. Hollingsworth and R.O. Dror, Molecular dynamics simulation for all, Neuron 2018, Volume 99, Issue 6, Pages 1129-1143.
[21] M.A. González, Force fields and molecular dynamics simulations, JDN 2011, Volume 12, Pages 169-200.
[22] S. Leonelli, Introduction: making sense of data-driven research in the biological and biomedical sciences, Stud Hist Philos Biol Biomed Sci 2012, Volume 43, Issue 1, Pages 1-3.
[23] C. Fluke and C. Jacobs, Surveying the reach and maturity of machine learning and artificial intelligence in astronomy, 2019.
[24] J.-P. Deranty and T. Corbin, Artificial intelligence and work: a critical review of recent research from the social sciences, AI & Society, 2022.

[25] M. Haenlein and A. Kaplan, A brief history of artificial intelligence: on the past, present, and future of artificial intelligence, California Management Review 2019, Volume 61, Issue 4, Pages 5-14.
[26] R.K. Vasudevan, K. Choudhary, A. Mehta, R. Smith, G. Kusne, F. Tavazza, L. Vlcek, M. Ziatdinov, S.V. Kalinin and J. Hattrick-Simpers, Materials science in the artificial intelligence age: high-throughput library generation, machine learning, and a pathway from correlations to the underpinning physics, MRS Communications 2019, Volume 9, Issue 3, Pages 821-838.
[27] G.K. Arun Baskarana, Krista Biggsb, Robert Hulla and Daniel Lewis, Adaptive characterization of microstructure dataset using a two-stage machine learning approach, Computational Materials Science 2020, Volume 177, Page 109593.
[28] S.M. Azimi, D. Britz, M. Engstler, M. Fritz and F. Mucklich, Advanced steel microstructural classification by deep learning methods, Scientific Reports 2018, Volume 8, Issue 1, Page 2128.
[29] R. Bostanabad, Y. Zhang, X. Li, T. Kearney, L.C. Brinson, D.W. Apley, W.K. Liu and W. Chen, Computational microstructure characterization and reconstruction: a review of the state-of-the-art techniques, Progress in Materials Science 2018, Volume 95, Pages 1-41.
[30] D.S. Bulgarevich, S. Tsukamoto, T. Kasuya, M. Demura and M. Watanabe, Pattern recognition with machine learning on optical microscopy images of typical metallurgical microstructures, Scientific Reports 2018, Volume 8, Issue 1, Pages 2078.
[31] R. Cang and M.Y. Ren, Deep network-based feature extraction and reconstruction of complex material microstructures, ASME 2016 International Design Engineering Technical Conferences and Computers and Information in Engineering Conference, 2016.
[32] A. Chowdhury, E. Kautz, B. Yener and D. Lewis, Image driven machine learning methods for microstructure recognition, Computational Materials Science 2016, Volume 123, Pages 176-187.
[33] I.D. Jung, D.S. Shin, D. Kim, J. Lee, M.S. Lee, H.J. Son, N.S. Reddy, M. Kim, S.K. Moon, K.T. Kim, J.-H. Yu, S. Kim, S.J. Park and H. Sung, Artificial intelligence for the prediction of tensile properties by using microstructural parameters in high strength steels, Materialia 2020, Volume 11, Pages 100699.
[34] E.J. Kautz, Predicting material microstructure evolution via data-driven machine learning, Patterns 2021, Volume 2, Issue 7, Pages 100285.

[35] J. Ling, M. Hutchinson, E. Antono, B. DeCost, E.A. Holm and B. Meredig, Building data-driven models with microstructural images: Generalization and interpretability, Materials Discovery 2017, Volume 10, Pages 19-28.
[36] A. Jain, S.P. Ong, G. Hautier, W. Chen, W.D. Richards, S. Dacek, S. Cholia, D. Gunter, D. Skinner, G. Ceder and K.A. Persson, Commentary: The materials project: A materials genome approach to accelerating materials innovation, APL Materials 2013, Volume 1, Issue 1.
[37] C. Kim, A. Chandrasekaran, T.D. Huan, D. Das and R. Ramprasad, Polymer genome: A data-powered polymer informatics platform for property predictions, The Journal of Physical Chemistry C 2018, Volume 122, Issue 31, Pages 17575-17585.
[38] J.E. Saal, S. Kirklin, M. Aykol, B. Meredig and C. Wolverton, Materials design and discovery with high-throughput density functional theory: the open quantum materials database (OQMD), J Jom 2013, Volume 65, Pages 1501-1509.
[39] J.J. de Pablo, N.E. Jackson, M.A. Webb, L.-Q. Chen, J.E. Moore, D. Morgan, R. Jacobs, T. Pollock, D.G. Schlom, E.S. Toberer, J. Analytis, I. Dabo, D.M. DeLongchamp, G.A. Fiete, G.M. Grason, G. Hautier, Y. Mo, K. Rajan, E.J. Reed, E. Rodriguez, V. Stevanovic, J. Suntivich, K. Thornton and J.-C. Zhao, New frontiers for the materials genome initiative, npj Computational Materials 2019, Volume 5, Issue 1, Pages 41.
[40] M. Gaultois, A. Oliynyk, A. Mar, T. Sparks, G. Mulholland and B. Meredig, Web-based machine learning models for real-time screening of thermoelectric materials properties, APL Materials 2016, Volume 4, Issue 5.
[41] A.A.K. Farizhandi, O. Betancourt and M. Mamivand, Deep learning approach for chemistry and processing history prediction from materials microstructure, Scientific Reports 2022, Volume 12, Issue 1, Pages 4552.
[42] S. Feng, H. Fu, H. Zhou, Y. Wu, Z. Lu and H. Dong, A general and transferable deep learning framework for predicting phase formation in materials, npj Computational Materials 2021, Volume 7, Issue 1, Pages 10.
[43] K. Baek, T. Hwang, W. Lee, H. Chung and M. Cho, Deep learning aided evaluation for electromechanical properties of complexly structured polymer nanocomposites, Composites Science and Technology 2022, Volume 228, Pages 109661.

[44] E. Champa-Bujaico, P. Garcia-Diaz and A.M. Diez-Pascual, Machine learning for property prediction and optimization of polymeric nanocomposites: a state-of-the-art, International Journal of Molecular Sciences 2022, Volume 23, Issue 18.
[45] J.B. Hooper and K.S. Schweizer, Theory of phase separation in polymer nanocomposites, Macromolecules 2006, Volume 39, Issue 15, Pages 5133-5142
[46] K. Müller, E. Bugnicourt, M. Latorre, M. Jorda, Y. Echegoyen Sanz, J.M. Lagaron, O. Miesbauer, A. Bianchin, S. Hankin, U. Bölz, G. Pérez, M. Jesdinszki, M. Lindner, Z. Scheuerer, S. Castelló and M. Schmid, Review on the processing and properties of polymer nanocomposites and nanocoatings and their applications in the packaging, Automotive and Solar Energy Fields, Nanomaterials 2017, Volume 7, Issue 4, Pages 74.
[47] B. Ashrafi, J.W. Guan, V. Mirjalili, Y.F. Zhang, L. Chun, P. Hubert, B. Simard, C.T. Kingston, O. Bourne and A. Johnston, Enhancement of mechanical performance of epoxy/carbon fibre laminate composites using single-walled carbon nanotubes, Composites Science and Technology 2011, Volume 71, Issue 13, Pages 1569-1578.
[48] F.H. Gojny, M.H.G. Wichmann, B. Fiedler, I.A. Kinloch, W. Bauhofer, A.H. Windle and K. Schulte, Evaluation and identification of electrical and thermal conduction mechanisms in carbon nanotube/epoxy composites, Polymer 2006, Volume 47, Issue 6, Pages 2036-2045.
[49] J. Njuguna and K. Pielichowski, Polymer nanocomposites for aerospace applications: properties, Advanced Engineering Materials 2003, Volume 5, Issue 11, Pages 769-778.
[50] M. Silva, N.M. Alves and M.C. Paiva, Graphene-polymer nanocomposites for biomedical applications, Polymers for Advanced Technologies 2018, Volume 29, Issue 2, Pages 687-700.
[51] S. Fu, Z. Sun, P. Huang, Y. Li and N. Hu, Some basic aspects of polymer nanocomposites: A critical review, Nano Materials Science 2019, Volume 1, Issue 1, Pages 2-30.
[52] B. Wetzel, F. Haupert and M. Qiu Zhang, Epoxy nanocomposites with high mechanical and tribological performance, Composites Science and Technology 2003, Volume 63, Issue 14, Pages 2055-2067.
[53] C. Li, Y. Nie, H. Zhan, J. Bai, T. Liu and Y. Gu, Mechanical properties of polymer nanocomposites with randomly dispersed and cross-linked two-dimensional diamond, Composites Science and Technology 2022, Volume 230, Pages 109722.
[54] N. Basavegowda, K.-H. Baek, Advances in Functional Biopolymer-Based Nanocomposites for Active Food Packaging Applications, Polymers 2021, Volume 13, Issue 23, Pages 4198.

[55] C. Zhang and S. Zheng, Morphology and fracture toughness of nanostructured epoxy resin containing aminoterminated poly(propylene oxide), Journal of Macromolecular Science, Part B 2010, Volume 49, Issue 3, Pages 574-591
[60] A.M. Turing, Computing Machinery and Intelligence, R. Epstein, G. Roberts and G. Beber (Edited), In: Parsing the Turing test: philosophical and methodological issues in the quest for the thinking computer, Springer Netherlands 2009, pages 23-65.
[61] A.L. Samuel, Some studies in machine learning using the game of checkers, IBM Journal of Research and Development 1959, Volume 3, Issue 3, Pages 210-229.
[62] A. Agrawal and A. Choudhary, Deep materials informatics: Applications of deep learning in materials science, MRS Communications 2019, Volume 9, Issue 3, Pages 779-792.
[63] J. Hill, G. Mulholland, K. Persson, R. Seshadri, C. Wolverton and B. Meredig, Materials science with large-scale data and informatics: Unlocking new opportunities, Mrs Bulletin 2016, Volume 41, Issue 5, Pages 399-409.
[64] Y. Lecun and Y. Bengio, Convolutional Networks for Images, Speech, and Time-Series, The handbook of brain theory and neural networks 1995 Volume 3361 Issue 10 Pages 1995.
[65] Y. LeCun, Y. Bengio and G. Hinton, Deep learning, nature 2015, Volume 521, Issue 7553, Pages 436-444.
[66] E.Z. Qu, A.M. Jimenez, S.K. Kumar and K. Zhang, Quantifying nanoparticle assembly states in a polymer matrix through deep learning, Macromolecules 2021, Volume 54, Issue 7, Pages 3034-3040.
[67] T. Wang, Z. Chen, Q. Shang, C. Ma, X. Chen, E. Xiao, A Promising and Challenging Approach: Radiologists' Perspective on Deep Learning and Artificial Intelligence for Fighting COVID-19, Diagnostics 2021, Volume 11, Issue 10, Pages 1924.
[68] K. Simonyan and A. Zisserman, Very deep convolutional networks for large-scale image recognition, arXiv preprint arXiv:1409.1556, 2014.
[69] Y. LeCun, L. Bottou, Y. Bengio and P. Haffner, Gradient-based learning applied to document recognition, Proceedings of the IEEE 1998, Volume 86, Issue 11, Pages 2278-2324.
[70] K. Ryan, J. Lengyel and M. Shatruk, Crystal structure prediction via deep learning, Journal of the American Chemical Society 2018, Volume 140, Issue 32, Pages 10158-10168.
[71] B. Fan, M. Zhou, C. Zhang, D. He and J. Bai, Polymer-based materials for achieving high energy density film capacitors, Progress in Polymer Science 2019, Volume 97, Pages 101143.

[72] Q. Liu, L. Seveyrat, F. Belhora and D. Guyomar, Investigation of polymer-coated nano silver/polyurethane nanocomposites for electromechanical applications, Journal of Polymer Research 2013, Volume 20, Issue 12.
[73] S.W. Ghori, R. Siakeng, M. Rasheed, N. Saba and M. Jawaid, The role of advanced polymer materials in aerospace, In: Sustainable composites for aerospace applications, Elsevier 2018.
[74] C.pelin, D. Ion, A. Stefan and G. Pelin, Nanocomposites as advanced materials for aerospace industry, Incas Bulletin 2012, Volume 4, Issue 4, Pages 73.
[75] X.T. Liu, Y.L. Guo, Y.Q. Ma, H.J. Chen, Z.P. Mao, H.L. Wang, G. Yu, and Y.Q. Liu, Flexible, Low-voltage and high-performance polymer thin-film transistors and their application in photo/thermal detectors, Advanced Materials 2014, Volume 26, Issue 22, Pages 3631-3636.
[76] F. Musil, S. De, J. Yang, J.E. Campbell, G.M. Day and M. Ceriotti, Machine learning for the structure-energy-property landscapes of molecular crystals, Chemical science 2018, Volume 9, Issue 5, Pages 1289-1300.
[77] Y.X. Wang, M. Zhang, A.Q. Lin, A. Iyer, A.S. Prasad, X.L. Li, Y.C. Zhang, L.S. Schadler, W. Chen and L.C. Brinson, Mining structure-property relationships in polymer nanocomposites using data-driven finite element analysis and multi-task convolutional neural networks, Molecular Systems Design & Engineering 2020, Volume 5, Issue 5, Pages 962-975.
[78] Le T-T., Prediction of tensile strength of polymer carbon nanotube composites using practical machine learning method, Journal of Composite Materials 2021, Volume 55, Issue 6, Pages 787-811.
[79] E.O. Pyzer-Knapp, C. Suh, R. Gómez-Bombarelli, J. Aguilera-Iparraguirre, A and Aspuru-Guzik, What is high-throughput virtual screening? A perspective from organic materials discovery, Annual Review of Materials Research 2015, Volume 45, Issue 1, Pages 195-216.
[80] M.M. Taye, Understanding of Machine Learning with Deep Learning: Architectures, Workflow, Applications and Future Directions, Computers 2023, Volume 12, Issue 5, Pages 91.
[81] B. Zazoum, E. Triki and A. Bachri, Modeling of mechanical properties of clay-reinforced polymer nanocomposites using deep neural network, Materials 2020, Volume 13, Issue 19, Pages 4266.
[82] A. Pratap, and N. Sardana, Machine learning-based image processing in materials science and engineering: A review, Materials Today: Proceedings 2022, Volume 62, Pages 7341-7347.

[83] B. Demirbay and D.B. Kara, Classification of opacity for polymer nanocomposite films via deep neural network (DNN) classifiers, 2022 International Conference on Innovations in Intelligent Systems and Applications (INISTA), IEEE, 2022, Pages 1-6.
[84] J. Jiang, Z.F. Zhang, J.Y. Fu, K.R. Ramakrishnan, C.Z. Wang and H.X. Wang, Machine learning assisted prediction of mechanical properties of graphene/aluminium nanocomposite based on molecular dynamics simulation, Materials & Design 2022, Volume 213.
[85] B. Liu, N. Vu-Bac and T. Rabczuk, A stochastic multiscale method for the prediction of the thermal conductivity of Polymer nanocomposites through hybrid machine learning algorithms, Composite Structures 2021, Volume 273, Pages 114269.
[86] L. Meli and P.F. Green, Aggregation and coarsening of ligand-stabilized gold nanoparticles in poly(methyl methacrylate) thin films, ACS Nano 2008, Volume 2, Issue 6, Pages 1305-1312.
[87] P. Mohan, A Critical Review: The Modification, Properties, and Applications of Epoxy Resins, Polymer-Plastics Technology and Engineering 2013, Volume 52, Issue 2, Pages 107-125.
[88] D.G. Papageorgiou, I.A. Kinloch, R.J. Young, Mechanical properties of graphene and graphene-based nanocomposites, Progress in Materials Science 2017, Volume 90, Pages 75-127.
[89] A.A. Balandin, Thermal properties of graphene and nanostructured carbon materials, Nature Materials 2011, Volume 10, Issue 8, Pages 569-581.
[90] M. Bhattacharya, Polymer Nanocomposites—A Comparison between Carbon Nanotubes, Graphene, and Clay as Nanofillers, Materials 2016, Volume 9, Issue 4, Pages 262.
[91] H. Zhang, X. Li , W. Qian , J. Zhu, B. Chen, J. Yang and Y. Xia, Characterization of mechanical properties of epoxy/nanohybrid composites by nanoindentation, Nanotechnology Reviews 2020, Volume 9, Issue 1, Pages 28-40.
[92] X. Li, W. Zhang, D. Li, J. Zhang, B. Long, Numerical Study on the Regression Method to Eliminate the Influence of Surface Morphology on Indentation Hardness of Thin Films, Coatings 2022, Volume 12, Issue 10, Pages 1447.
[93] R. Poveda, N. Gupta and M. Porfiri, Poisson's ratio of hollow particle filled composites, Materials Letters 2010, Volume 64, Pages 2360-2362.
[94] W.C. Oliver, G.M. Pharr, An improved technique for determining hardness and elastic modulus using load and displacement sensing indentation experiments, Journal of Materials Research 1992, Volume 7, Issue 6, Pages 1564-1583.

[95] J. Cho, J.J. Luo, I.M. Daniel, Mechanical characterization of graphite/epoxy nanocomposites by multi-scale analysis, Compos Sci Technol 2007, Volume 67, Issue 11, Pages 2399-2407.
[96] M. Abraham, D.V. Claudio, S. Stefano, A. Alidad,J. W. Drelich, Contact angles and wettability: towards common and accurate terminology, Surface Innovations 2017, Volume 5, Issue 1, Pages 3-8.
[97] L. Makkonen, Young's equation revisited, Journal of Physics: Condensed Matter 2016, Volume 28, Issue 13, Pages 135001.
[98] A. A. K. Farizhandi, O. Betancourt and M. Mamivand, Deep Learning approach for chemistry and processing history prediction from materials microstructure, Scientific Reports 2022, Volume 12, Issue 1, Pages 4552.
[99] D. Jha, K. Choudhary, F. Tavazza, W.-k. Liao, A. Choudhary, C. Campbell and A. Agrawal, Enhancing materials property prediction by leveraging computational and experimental data using deep transfer learning, Nature Communications 2019, Volume 10, Page 5316.
[100] C. Shorten, T. M. Khoshgoftaar, A survey on image data augmentation for deep learning, Journal of Big Data 2019, Volume 6, Issue 1, Pages 60.
[101] A. Mikołajczyk and M. Grochowski, Data augmentation for improving deep learning in image classification problem, 2018 International Interdisciplinary PhD Workshop (IIPhDW), 2018, Pages 117-122.
[102] F.a.o. Chollet, Keras, GitHub, 2015.
[103] K. Fukushima, Cognitron: A self-organizing multilayered neural network, Biological Cybernetics, 1975, Volume 20, Issue 3, Pages 121-136.
[104] A.F. Agarap, Deep learning using rectified linear units (relu), arXiv preprint arXiv:1803.08375, 2018.
[105] D. Kingma and J. Ba, Adam: A Method for Stochastic Optimization, arXiv preprint arXiv:1412.6980, 2014.
[106] K.M. Ting, Confusion matrix, Encyclopedia of Machine Learning and Data Mining, 2017, Volume 260.
[107] C. Goutte and E. Gaussier, A Probabilistic Interpretation of Precision, Recall and F-Score, with Implication for Evaluation, Advances in Information Retrieval, 2005, Volume 3408.

[108] M.A. Butt, Thin-Film Coating Methods: A Successful Marriage of High-Quality and Cost-Effectiveness—A Brief Exploration, Coatings 2022, Volume 12, Issue 8, Pages 1115.
[109] A. Azapagic, A. Emsley, I. Hamerton, Managing Polymer Waste: Technologies for Separation and Recycling, Polymers, the Environment and Sustainable Development, In: Polymers, the Environment and Sustainable Development 2003, Pages. 79-99.
[110] J. Choi, B. Lim, Y. Yoo, Advancing Plastic Waste Classification and Recycling Efficiency: Integrating Image Sensors and Deep Learning Algorithms, Applied Sciences 2023, Volume 13, Issue 18, Pages 10224.